

REVIEWS OF TOPICAL PROBLEMS

PACS numbers: 41.75.Ht, **52.60.+h**, 52.70.Gw

Problems in the theory of relativistic plasma microwave electronics

M Birau, M A Krasil'nikov, M V Kuzelev, A A Rukhadze

Contents

1. Introduction **975**
2. Initial assumptions and equations **976**
3. Plasma waves **977**
4. Linear theory of the amplification of plasma waves by a relativistic electron beam **978**
5. Generation **983**
6. Efficiency of a plasma microwave amplifier **984**
7. Nonlinear equations for a plasma amplifier **985**
8. Spatial dynamics of amplification and the spectra of a plasma amplifier **987**
9. Conclusion **991**
References **991**

Abstract. A review of the theoretical studies on wide-band microwave sources employing the stimulated Cherenkov radiation of relativistic electron beams in a plasma waveguide is presented. The motivation for such studies lies in recent experiments on microwave plasma noise sources using intense relativistic electron beams. Although only theoretical problems are discussed, all the necessary estimates are obtained using parameter values taken from actual General Physics Institute experiments, in part already published. A very incomplete preliminary comparison of theoretical and experimental results is given.

1. Introduction

Relativistic plasma microwave electronics, both theoretical and experimental, has been in existence for over 25 years. From time to time over these years we, in different combinations, have been publishing reviews of the achievements of this science on the pages of *Physics – Uspekhi* [1 – 4] and elsewhere [5 – 8]†. In almost every review we wrote that "plasma microwave electronics as a science was conceived in 1949 after the pioneering works of A I Akhiezer and Ya B Feinberg [11], and D Bohm and E Gross [12], who predicted the effect of beam instability in plasma". The results of these first and many subsequent studies at the initial stage of theoretical plasma microwave electronics are summarized in reviews [13, 14]‡.

Much later it transpired that the effect of beam instability in plasma has many mechanisms and manifestations. It was discovered, for example, that of special interest for the construction of sources of electromagnetic microwaves are the instabilities caused by the electron beam of proper plasma electromagnetic oscillations stimulated by Cherenkov emission. Depending on the density of the beam, the stimulated emission may be either the wave – particle effect (single-particle Cherenkov effect), or the wave – wave effect (collective Cherenkov effect) [4, 8, 16]§. In addition, it turned out that because of the negative dielectric permittivity of plasma the electron beam may become unstable irrespective of any emission processes [18 – 21]. By the early 1980s, as duly noted in our review [2], the theoreticians for the most part had masterminded these and many other intricate and complex features of beam instability in plasma. The next stage was concerned with the development of a consistent nonlinear theory and the complex of methods and approaches capable of explaining and even predicting the results of modern experiments. It ought to be noted that the first works on the nonlinear theory of the beam – plasma interaction were carried out much earlier [22 – 25]. The results of these early studies relate mainly to the interaction of weakly relativistic electron beams with potential oscillations of plasma — that is, to a case of little interest for relativistic plasma microwave electronics.

Concurrently with the theory was developed the experiment on the excitation of electromagnetic waves in plasma by an electron beam, and their emission from the plasma. The initial numerous experiments carried out in the 1950s and 60s revealed, however, that the intensity of this emission is low. Later it became clear that it was not the low efficiency that mattered, but rather the electron beam being non-relativistic.

† See also monographs [9, 10].

‡ See also monograph [15].

§ See also monograph [17].

M Birau LPMI, Ecole Polytechnique, Palaiseau, France
Tel. 33 (1) 69 33 32 74
Fax 33 (1) 69 33 30 23
E-mail: birau@lpmi.polytechnique.fr
M A Krasil'nikov, M V Kuzelev Moscow State University of Printing Art
ul. Pryanishnikova 2a, 127550 Moscow, Russia
Tel. (7-095) 976 40 88. Fax (7-095) 976 06 35
A A Rukhadze General Physics Institute, Russian Academy of Sciences
ul. Vavilova 38, 117942 Moscow, Russia
Tel. (7-095) 135 02 47. Fax (7-095) 135 02 70

Received 26 November 1996, revised 18 March 1997
Uspekhi Fizicheskikh Nauk **167** (10) 1025 – 1042 (1997)
Translated by A S Dobroslavskiĭ; edited by A Yaremchuk

The waves excited with such beams were highly potential, and therefore were poorly emitted from the bulk of the plasma. An excellent historical review of this non-relativistic period of plasma microwave electronics can be found in Ref. [26].

Pulsed sources of dense relativistic electron beams were developed in the late 1960s and early 70s, and immediately found diverse applications in science and technology, including microwave electronics [27, 28] †. Relativistic microwave electronics was born in 1972, when the joint efforts of IOFAN (then FIAN) and IPFAN (then NIRFI) resulted in the development of the first sufficiently efficient Cherenkov microwave generator of the backward-wave tube type using a relativistic electron beam [31] ‡. However this generator used stimulated Cherenkov emission of a dense beam of relativistic electrons in a vacuum retarding structure, and thus pertained to the devices of relativistic vacuum microwave electronics. The achievements of relativistic vacuum microwave electronics are described in detail in Ref. [33] and collected papers [34].

The first plasma microwave generator based on the stimulated Cherenkov emission of a relativistic electron beam in a plasma waveguide (a traveling wave tube) appeared later, in 1982, and was extensively studied in experiments [6, 34 – 37] carried out mainly in IOFAN.

Experimental studies were preceded by theoretical works [38 – 40], which laid down the main principles of plasma relativistic microwave electronics. These and subsequent papers [2 – 5, 8, 10] pointed out the main advantages of the relativistic Cherenkov plasma microwave sources over the traditional vacuum sources like traveling and backward wave tubes. These advantages include, in particular, the possibility to adjust the frequency of radiation relatively easily by changing the density of the plasma, and to construct both narrow-band (almost monochromatic) and broad-band (noise-like) microwave sources realizing either the one-particle or the collective mechanisms of stimulated Cherenkov emission of plasma electromagnetic waves by the relativistic electron beam. These advantages today are not just theoretical, they have been demonstrated in experiments [6, 7, 41, 42].

Another proof of the superiority of the plasma sources of microwave radiation was given by the recent results of a theoretical analysis of their efficiency. As demonstrated in Refs [43 – 46], the use of diodes with magnetic insulation in relativistic plasma microwave amplifiers automatically results in the optimum emission efficiency (about 20%), which remains practically unchanged when the energy of the electrons in the beam is above 1 MeV (given, of course, that the length of the amplifier is sufficient). Because of its importance, the problem of efficiency will be discussed in greater detail later on.

The important advantages also include the feasibility of long-pulse generation and amplification of high-power microwave radiation in plasma sources. This is possible because the strong high-frequency field of plasma waves is separated from metallic surfaces, and there are no breakdowns on the walls of 'retarding' structures, which are the stumbling blocks for high-power vacuum sources of microwaves [47 – 50] (see also collected papers [34]).

It should be observed that until recently the main emphasis in experimental works on the excitation of microwave radiation in plasma was governed by the desire to produce narrow-band coherent radiation with an efficiency as high as possible, and to move towards shorter wavelengths, from centimeters to millimeters. Naturally, the same was the direction of theoretical research, which was mainly concerned with single-mode (or single-wave) monochromatic (or quasi-monochromatic) plasma-beam microwave sources. It is precisely such sources that are dealt with in the reviews quoted above (see also Refs [5 – 10]). Recent experimental studies [41, 42] indicate, however, that for various reasons the emission spectrum of plasma microwave sources may broaden. The broadening of the emission spectrum may be induced, for example, by raising the current in the beam and generally by increasing the radiated power. The specific dispersion law of plasma waves (which is almost linear in the non-potential range) by itself facilitates excitation of these waves over a broad frequency range. In other words, the experimental works of recent years have paved the way towards the construction of high-power broad-band noise sources of microwaves, based on the stimulated Cherenkov emission of high-current relativistic electron beams in plasma.

Theory did not fall behind experiment. The broadening of the emission spectrum resulting from the nonlinearity of the beam (the generation of harmonics of the principal mode of the microwave field), the high beam current and the geometry of the beam – plasma system (the transition from the single-particle wave – particle regime to the collective wave – wave regime), the capture of a large number of longitudinal modes into the amplification band, the transverse non-unimodality of stimulated emission, and the nonlinear frequency shift of beam and plasma waves was studied in Refs [43 – 45, 51, 52]. The comparison between theoretical and experimental [41, 42] results qualitatively confirms the validity of the theoretical developments and, even though such a comparison is not yet complete (mainly because of the insufficiency of experimental data available today), we decided to present this review of the results of these theoretical works tied in with the real conditions of particular experiments. This work is mainly focused on the problem of amplification of microwaves in plasma. The problem of generation has been treated in the theoretical papers [44, 45, 53]. As far as the experiments are concerned, at least the latest ones, it is most likely that a plasma microwave amplifier was realized in Ref. [41], and a generator in Ref. [42]. Thus, we now have some experimental material available for comparison with the theoretical results.

2. Initial assumptions and equations

Assume that a relativistic electron beam propagates along the axis of a metallic waveguide. The beam is injected into the waveguide in the plane $Z = 0$ (the Z axis coincides with the axis of the waveguide), and the collector is located at $Z = L$ where the horn begins for letting the radiation out. The beam is injected strictly along the axis of the waveguide, which is filled with plasma. In the unperturbed state the densities of the beam and the plasma do not depend on Z. In the transverse direction, however, their densities are not uniform. Both the beam and the plasma are cold, the static charge and current of the beam are neutralized, and the slow motion of the plasma ions is disregarded. Assume also that

† See also monographs [9, 29, 30].

‡ The experimental parameters were as follows: output radiation power up to 300 W, pulse length about 20 ns, efficiency of generator about 14%, wavelength 3 cm. Almost immediately these results were reproduced in the United States [32].

the motion of plasma electrons is described by linear equations, and there is a strong external longitudinal magnetic field which only permits the beam and plasma electrons to move along the Z-axis. The validity of these assumptions and the possible results of their violation are discussed, for example, in Refs [10, 24, 25, 54, 55] and the literature quoted therein.

In a strong external longitudinal magnetic field the beam and plasma electrons are only affected by those field perturbations whose longitudinal electric component is nonzero. Such perturbations include the E (or TM) waves with which we are concerned in this study. It is convenient to describe the field of such waves in terms of the polarization potential ψ which satisfies the following equation [56, 57]:

$$\frac{\partial}{\partial t}\left(\Delta_{\perp}+\frac{\partial^2}{\partial z^2}-\frac{1}{c^2}\frac{\partial^2}{\partial t^2}\right)\psi=-4\pi(j_{bz}+j_{pz})\,. \tag{2.1}$$

Here j_{bz} and j_{pz} are the perturbations of the longitudinal current densities in the beam and the plasma, respectively, and $\Delta_{\perp}$ is the transverse component of the Laplace operator. The perturbations of the current densities are conveniently represented as

$$j_{pz}=P_{p}(\mathbf{r}_{\perp})\,j_{p}\,,\qquad j_{bz}=P_{b}(\mathbf{r}_{\perp})\,j_{b}\,, \tag{2.2}$$

where $P_p(\mathbf{r}_{\perp})$ and $P_b(\mathbf{r}_{\perp})$ are the functions which describe the transverse density profiles, and $\mathbf{r}_{\perp}$ is the coordinate in the transverse cross section of the waveguide.

The equation for j_p follows from the linearized equations of the cold hydrodynamics of plasma electrons [58] and has the form

$$\frac{\partial j_p}{\partial t}=\frac{\omega_p^2}{4\pi}\,E_z\,. \tag{2.3}$$

Here

$$E_z=\left(\frac{\partial^2}{\partial z^2}-\frac{1}{c^2}\frac{\partial^2}{\partial t^2}\right)\psi \tag{2.4}$$

is the longitudinal component of the electric field, and ω_p is the Langmuir frequency of plasma electrons [it does not depend on the transverse coordinate, since this dependence is already included in the first relation in Eqn (2.2)].

Now let us formulate the equations for the perturbation of the beam current density. Let t_0 be the time of injection of another electron beam into the waveguide through the plane $Z=0$ (the injection velocity is the same for all electrons). Using the Liouville theorem of conservation of phase volume and the formal solution of the Vlasov equation [59] one may demonstrate that the density of current in any cross section $Z>0$ is given by [23, 25]

$$j_b=en_b\int v(z,t_0)\,\delta\big[t-t(z,t_0)\big]\,\mathrm{d}t_0\,, \tag{2.5}$$

where n_b is the density of the beam electrons (by virtue of the second relation in Eqn (2.2) this density also does not depend on the transverse coordinate $\mathbf{r}_{\perp}$), and $v(z,t_0)$, $t(z,t_0)$ are the solutions of the characteristic set of Vlasov equations

$$\begin{aligned}&\frac{\mathrm{d}t}{\mathrm{d}z}=\frac{1}{v}\,,\\&v\,\frac{\mathrm{d}v}{\mathrm{d}z}=\frac{e}{m}\left(1-\frac{v^2}{c^2}\right)^{3/2}E_z\,.\end{aligned} \tag{2.6}$$

The system (2.6) is solved with the initial conditions $t(z=0)=t_0$, $v(z=0)=u$, where u is the beam velocity at injection†.

Equations (2.1)–(2.6) form the basis of the theory presented in this paper.

3. Plasma waves

Consider the frequency spectra of the simplest plasma waves. To do this we only need equations (2.1) and (2.3) with zero beam current. The equations being linear, their solution may be sought in the form

$$(j_p,\psi)=\big[\tilde{j}_p(\mathbf{r}_{\perp}),\tilde{\psi}(\mathbf{r}_{\perp})\big]\exp(-\mathrm{i}\omega t+\mathrm{i}k_z z)\,, \tag{3.1}$$

where ω is the frequency, k_z is the longitudinal wave number, and $\tilde{j}_p$ and $\tilde{\psi}$ are functions of only the transverse coordinate.

Let $\varphi_n(\mathbf{r}_{\perp})$ be the eigenfunctions of the transverse cross section of the waveguide ($n=1,2,\ldots$), and $k_{\perp n}^2$ the corresponding eigenvalues. The eigenfunctions and eigenvalues satisfy the equation

$$\Delta_{\perp}\varphi_n=-k_{\perp n}^2\varphi_n\,.$$

Now we expand $\tilde{\psi}$ in the eigenfunctions, express the expansion coefficients from Eqn (2.1), and substitute them into Eqn (2.3), getting as a result the following integral equation for $\tilde{j}_p$:

$$\begin{aligned}&\omega^2\tilde{j}_p(\mathbf{r}_{\perp})=\omega_p^2\int_{S_w}K_p(\mathbf{r}_{\perp},\mathbf{r}_{\perp}^*)\,\tilde{j}_p(\mathbf{r}_{\perp}^*)\,\mathrm{d}\mathbf{r}_{\perp}^*\,,\\&K_p(\mathbf{r}_{\perp},\mathbf{r}_{\perp}^*)=\sum_{n=1}^{\infty}\frac{\chi^2}{k_{\perp n}^2+\chi^2}\,\frac{P_p(\mathbf{r}_{\perp}^*)\varphi_n(\mathbf{r}_{\perp}^*)\varphi_n(\mathbf{r}_{\perp})}{\|\varphi_n\|^2}\,.\end{aligned} \tag{3.2}$$

Here $\chi^2=k_z^2-\omega^2/c^2$; S_w is the transverse cross section of the waveguide, and $\|\varphi_n\|$ is the norm of the eigenfunction. The condition of solvability of Eqn (3.2) is the dispersion equation for finding the frequency spectra of plasma waves in a completely magnetized plasma waveguide in the most general but implicit form.

With reference to real experiments [6, 35–37, 41, 42], let us specify the geometry: a circular waveguide of radius R which contains a thin annular plasma of thickness Δ_p and mean radius $r_p<R$. In the theoretical model it is expedient to assume that the plasma is not just thin but infinitesimally thin [61], with a transverse density profile $P_p=\Delta_p\delta(r-r_p)$, where r is the coordinate along the radius of the waveguide. Later on we shall discuss the implications of replacing the real transverse profile of the plasma with the infinitely thin profile.

Since the eigenfunctions for the round waveguide are the Bessel functions, after some cumbersome algebra (see, for example, Ref. [62]), from Eqn (3.2) we get the explicit dispersion equation in the form

$$D_p\equiv\omega^2-\omega_p^2\,\frac{\chi^2}{k_{\perp p}^2}=0\,, \tag{3.3}$$

$$k_{\perp p}^2=\left\{r_p\Delta_p I_l^2(\chi r_p)\left[\frac{K_l(\chi r_p)}{I_l(\chi r_p)}-\frac{K_l(\chi R)}{I_l(\chi R)}\right]\right\}^{-1}\,, \tag{3.4}$$

† A rigorous derivation of Eqn (2.5) and the limits of its applicability can be found in the methodological paper [60].

where I_l, K_l are the modified Bessel function and the MacDonald function, respectively, and $l = 0, 1, \ldots$ is the azimuthal wave number†. At $\omega < k_z c$ formulas (3.3) and (3.4) define the frequency spectra of the surface plasma waves, and Eqn (3.4) represents the squared transverse wave number of these waves.

Consider now the frequency spectra of surface plasma waves for different wavelengths. In the long-wave limit, when $k_z \to 0$, from Eqn (3.3) we get

$$\omega = \omega_{\mathrm{p}} \frac{k_z c}{\sqrt{k_{\perp\mathrm{p}}^2 c^2 + \omega_{\mathrm{p}}^2}} , \tag{3.5}$$

where, as follows from Eqn (3.4), the transverse wave number is given by

$$k_{\perp\mathrm{p}}^2 = \begin{cases} \left[r_{\mathrm{p}} \Delta_{\mathrm{p}} \ln \dfrac{R}{r_{\mathrm{p}}} \right]^{-1} , & l = 0 , \\ 2l \left\{ r_{\mathrm{p}} \Delta_{\mathrm{p}} \left[1 - \left(\dfrac{r_{\mathrm{p}}}{R} \right)^{2l} \right] \right\}^{-1} , & l = 1, 2, \ldots \end{cases} \tag{3.6}$$

At shorter wavelengths, of the order of the radius of the plasma tube r_{p}, the frequency spectrum is given by (as for deep-water waves)

$$\omega = \omega_{\mathrm{p}} \left(\frac{k_z \Delta_{\mathrm{p}}}{2} \right)^{1/2} . \tag{3.7}$$

In the range of wavelengths where the spectrum is described by Eqn (3.6), the longitudinal component of the electric field of a surface wave falls off very rapidly (exponentially) from the surface of the plasma tube to the vacuum.

Finally, at wavelengths below Δ_{p} ($k_z \Delta_{\mathrm{p}} \geqslant 1$) the model of an infinitely thin plasma is simply not valid, because it does not take into account the confinement of the fields of the wave within the plasma tube. If the finite thickness of the plasma is taken into account, we find that $\omega \to \omega_{\mathrm{p}}$ as $k_z \to \infty$, as ought to be expected. However, this only happens when the plasma wave becomes highly potential and its Cherenkov excitation by the electron beam is of no interest for relativistic plasma microwave electronics.

There is yet another circumstance associated with the finite thickness of the plasma. As follows from Eqns (3.3) and (3.4), each azimuthal wave number l in the model of an infinitely thin plasma corresponds to a unique surface wave with a squared transverse wave number (in the long-wave limit) of the order of $(r_{\mathrm{p}} \Delta_{\mathrm{p}})^{-1}$. In addition to these waves, a finite-thickness plasma also contains oscillations always confined in the bulk. The estimated squared transverse wave number of oscillations confined in the bulk is about Δ_{p}^{-2}, which is much greater than the value given by Eqn (3.6) when $\Delta_{\mathrm{p}} \ll r_{\mathrm{p}}$. Hence it follows that the phase velocities of the waves confined in the bulk are low, and they cannot be Cherenkov-excited by a relativistic electron beam. This is the reason why the finite thickness of the plasma may be disregarded in the study of the Cherenkov interaction of a relativistic electron beam with a thin tubular plasma.

Figure 1 shows the dispersion curve for the spectrum of oscillations of a symmetrical ($l = 0$) surface wave in an infinitely thin plasma (curve *1*). The curve is plotted for the following parameters: radius of the waveguide — 1.8 cm, average plasma radius — 1.0 cm, plasma thickness — 0.1 cm, plasma frequency — 35×10^{10} radians per second. The initial (the steepest) portion of the curve is described by Eqn (3.5). The corresponding wave is referred to as the plasma cable wave [7, 61]. The dispersion law for the next portion of the curve is given by Eqn (3.7). As the plasma frequency is approached, the curve ceases to be correct: the finite thickness of the plasma must be taken into account.

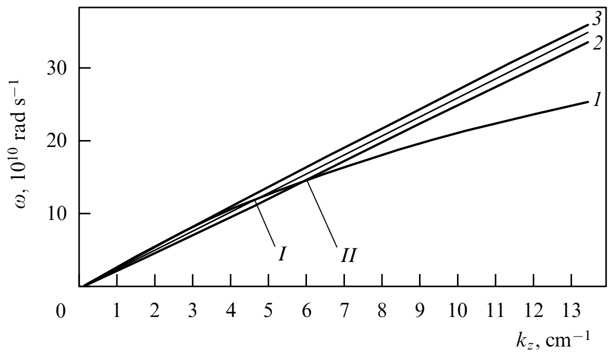

Figure 1. Spectra of oscillations in a waveguide with a magnetized thin plasma and electron beam (neglecting the interaction between plasma and beam): plasma wave (curve *1*); slow beam wave (curve *2*); fast beam wave (curve *3*); one-particle Cherenkov resonance (point *I*); collective Cherenkov resonance (point *II*).

Figure 1 also features the straight line of the Cherenkov resonance $\omega = k_z u$ (for the beam velocity of $u = 2.6 \times 10^{10}$ cm s^{-1}) and the point of the single-particle Cherenkov resonance (wave-particle resonance) of the electron beam with the surface plasma wave (point *I*). From Fig. 1 we see that as the plasma frequency decreases (with increasing velocity of the beam) the frequency of the Cherenkov resonance goes down and becomes zero at a certain threshold value. This threshold value can be found by substituting $\omega = k_z u$ into Eqn (3.5),

$$\omega_{\mathrm{p}}^2 = k_{\perp\mathrm{p}}^2 u^2 \gamma^2 , \tag{3.8}$$

where $\gamma = (1 - u^2/c^2)^{-1/2}$ is the relativistic factor for the electrons of the beam. The threshold (3.8) depends on the azimuthal wave number l. As follows from Eqn (3.6), the lowest threshold value corresponds to the mode with $l = 0$.

If the plasma frequency is below the threshold, single-particle Cherenkov resonance is not possible. The absence of a resonance, however, does not preclude the existence of stimulated Cherenkov emission, or the stability of the beam in the plasma. As will be shown below, the threshold is much lower than that given by Eqn (3.8) when the density of the beam is high.

4. Linear theory of the amplification of plasma waves by a relativistic electron beam

In the linear approximation it is more convenient to use the equations of cold magnetohydrodynamics in place of Eqns (2.5) and (2.6) for the description of the beam. In this way it is easy to obtain one equation for j_{b} from Eqn (2.2):

$$\left(\frac{\partial}{\partial t} + u \frac{\partial}{\partial z} \right)^2 j_{\mathrm{b}} = \frac{\omega_{\mathrm{b}}^2 \gamma^{-3}}{4\pi} \frac{\partial E_z}{\partial t} . \tag{4.1}$$

† In obtaining Eqns (3.3) and (3.4) one must take into account that the integrals with respect to radius in Eqn (3.2) can be calculated exactly, since in the case of an infinitely thin plasma they contain delta-functions.

The latter is the counterpart of Eqn (2.3), and $\omega_b = (4\pi e^2 n_b m^{-1})^{1/2}$ is the Langmuir frequency of the electrons of the beam. Assuming in the linear approximation [see Eqn (3.1)] that

$$j_b = \tilde{j}_b(\mathbf{r}_\perp)\exp(-i\omega t + ik_z z)\,,$$

by analogy with Eqn (3.2) we get from Eqns (2.1)–(2.4) and (4.3) the following set of integral equations for $\tilde{j}_p$ and $\tilde{j}_b$:

$$\begin{aligned}
&\omega^2 \tilde{j}_p(\mathbf{r}_\perp) - \omega_p^2 \int_{S_w} K_p(\mathbf{r}_\perp, \mathbf{r}_\perp^*)\,\tilde{j}_p(\mathbf{r}_\perp^*)\,d\mathbf{r}_\perp^* \\
&\qquad = \omega_b^2 \gamma^{-3} \int_{S_w} K_b(\mathbf{r}_\perp, \mathbf{r}_\perp^*)\,\tilde{j}_b(\mathbf{r}_\perp^*)\,d\mathbf{r}_\perp^*\,, \\
&(\omega - k_z u)^2 \tilde{j}_b(\mathbf{r}_\perp) - \omega_b^2 \gamma^{-3} \int_{S_w} K_b(\mathbf{r}_\perp, \mathbf{r}_\perp^*)\,\tilde{j}_b(\mathbf{r}_\perp^*)\,d\mathbf{r}_\perp^* \\
&\qquad = \omega_p^2 \int_{S_w} K_p(\mathbf{r}_\perp, \mathbf{r}_\perp^*)\,\tilde{j}_p(\mathbf{r}_\perp^*)\,d\mathbf{r}_\perp^*\,.
\end{aligned} \tag{4.2}$$

The condition of solvability of the set (4.2) is the dispersion equation for finding the complex spectra of the beam-plasma system. The quantity K_p in Eqn (4.2) coincides with the second expression in Eqn (3.2). The same expression with $P_p(\mathbf{r}_\perp^*)$ replaced by $P_b(\mathbf{r}_\perp^*)$ defines the quantity K_b.

Before analyzing the general equation, let us consider the spectra of only the beam waves in the absence of plasma. For this we need the second equation of Eqn (4.2) with $\omega_p = 0$. To be consistent with the experimental conditions, we assume that the electron beam is, like the plasma, also thin annular, and its density profile is $P_b = \Delta_b \delta(r - r_b)$, where Δ_b is the thickness of the beam, and r_b is its mean radius. In exactly the same way as the dispersion equation (3.3) was derived, we get

$$D_b \equiv (\omega - k_z u)^2 - \omega_b^2 \gamma^{-3} \frac{\chi^2}{k_{\perp b}^2} = 0\,, \tag{4.3}$$

where $k_{\perp b}$ is the beam counterpart of $k_{\perp p}$ in Eqn (3.4). To find $k_{\perp b}$ from the expression for $k_{\perp p}$ we have to replace the subscript 'p' (for plasma) in the latter by the subscript 'b' (for beam).

In addition to the plasma curves, Fig. 1 also displays the dispersion curves for the spectra of waves of an infinitely thin tubular beam in a circular waveguide (recall that the interaction between the beam and the plasma in this diagram has not yet been taken into account). The dispersion curves were plotted for the following parameters: waveguide radius — 1.8 cm; mean radius of the beam — 0.65 cm; thickness of the beam — 0.1 cm; current — 2 kA; relativistic factor — $\gamma = 2$; $l = 0$. The wave with the higher phase velocity (corresponding to curve *3*) is called the fast wave, and the wave with the lower phase velocity (curve *2*) is referred to as the slow space charge wave. The energy of the slow wave of the beam is negative, which leads to the instability of the beam in the plasma [16, 63].

When the finite thickness of the beam is taken into account, curves *2* and *3* in Fig. 1 are supplemented by the curves pressed closer to the Cherenkov resonance line $\omega = k_z u$. They correspond to the higher radial modes of space charge, confined in the bulk of the beam. Later on we shall discuss the effect of these modes on the characteristics of beam-plasma interaction.

The intercept (point *II*) of the dispersion curve of the plasma wave and the dispersion curve of the slow beam wave (point *II* in Fig. 1) is the point of collective Cherenkov resonance (wave–wave resonance).

Now let us go over to the general equations (4.2). We assume that both the beam and the plasma are infinitely thin. We multiply the first equation in Eqn (4.2) by $\delta(r - r_p)$, the second by $\delta(r - r_b)$, and integrate with the weight r from zero to R. Eliminating $\tilde{j}_p(r_p)$, $\tilde{j}_b(r_b)$, we get the following dispersion equation of the linear theory of beam–plasma interaction:

$$D_p D_b = \Theta \omega_p^2 \frac{\chi^2}{k_{\perp p}^2}\, \omega_b^2 \gamma^{-3} \frac{\chi^2}{k_{\perp b}^2}\,. \tag{4.4}$$

From Eqn (4.4) we see that the beam-plasma interaction is indeed the interaction between the beam waves (4.3) and the plasma waves (4.4). The efficiency of this interaction is defined by the coupling coefficient Θ on the right-hand side of Eqn (4.4). The coupling coefficient depends on the frequency (and the longitudinal wave number), the mean radius of the beam, and the mean radius of the plasma. If the beam and the plasma are perfectly aligned in the cross section of the waveguide, the coupling coefficient is equal to unity. Otherwise the coupling coefficient is less than one, and reduces with increasing frequency. Physically, the coupling coefficient shows how far the field of the beam wave penetrates into the plasma, and how far the field of the plasma wave penetrates into the beam. We do not quote here the general expression for Θ because of its complexity (for details see Ref. [62]), and will confine ourselves to two extreme cases.

For the round waveguide under consideration with an infinitely thin annular beam and the plasma in the low-frequency limit the coupling coefficient is given by (for definiteness, $r_b \leqslant r_p$ and $l = 0$):

$$\Theta = \frac{\ln(R/r_p)}{\ln(R/r_b)}\,. \tag{4.5}$$

In the opposite high-frequency limit the asymptotic expression is

$$\Theta = \exp\bigl(-2\chi|r_p - r_b|\bigr)\,. \tag{4.6}$$

In the first approximation χ may mean $\omega/(u\gamma)$, since the Cherenkov instability corresponds to $k_z \approx \omega/u$.

Being mainly concerned with the problem of amplification, we seek a solution of the dispersion equation (4.4) in the form

$$k_z = \frac{\omega}{u}(1 + \delta)\,, \tag{4.7}$$

where δ is the dimensionless complex gain coefficient. Since the density of the beam is actually always less than the density of the plasma, we have $|\delta| \ll 1$. Substituting Eqn (4.7) into Eqn (4.4), after some straightforward algebra we get a cubic equation which takes into account the effects associated both with the high beam current and the non-potentiality of the beam and plasma waves:

$$\begin{aligned}
&\bigl[1 - \alpha_p(1 + 2\gamma^2\delta)\bigr]\bigl[\delta^2 - \alpha_b(1 + 2\gamma^2\delta)\bigr] \\
&\qquad = \Theta \alpha_p \alpha_b (1 + 2\gamma^2\delta)^2\,.
\end{aligned} \tag{4.8}$$

Here

$$\alpha_p = \frac{\omega_p^2}{k_{\perp p}^2 u^2 \gamma^2}\,, \qquad \alpha_b = \frac{\omega_b^2 \gamma^{-3}}{k_{\perp b}^2 u^2 \gamma^2} \tag{4.9}$$

are the 'density' parameters which, like the coupling coefficient, only depend on $\omega/(u\gamma)$ (through squared transverse wave numbers). Equation (4.8) is derived for the case $\omega \ll \omega_p$, when the dispersion of the surface plasma wave is close to linear. Equation (4.8) can also be extended to the range of higher frequencies. We are not going to do this here to avoid cumbersome mathematics (see Ref. [62]). Instead, we shall show an easy qualitatively sound way of taking the real dispersion of plasma waves into account at any frequencies up to ω_p using the simple equation (4.8).

The nulls of the brackets on the left-hand side of Eqn (4.8) define the longitudinal wave numbers [with the replacement of variable (4.7)] of the plasma wave traveling in the same direction as the beam, the fast beam wave and the slow beam wave. The fast wave is of no interest for our further discussion. For the plasma wave we have

$$\delta_p = \frac{1}{2\gamma^2}\left(\frac{1}{\alpha_p} - 1\right), \tag{4.10}$$

and for the slow beam wave we get

$$\delta_b^- = \sqrt{\alpha_b + \gamma^4\alpha_b^2} + \gamma^2\alpha_b . \tag{4.11}$$

Observe that by its properties the slow beam wave is in fact potential if $\gamma^2\sqrt{\alpha_b}$ is much less than one; then the wave number of the slow wave is $\delta_b^- = \sqrt{\alpha_b}$. The parameter $\gamma^2\sqrt{\alpha_b}$ will be specially discussed later on.

As noted above, when the finite thickness of the plasma is taken into account we should have $k_z \to \infty$ at $\omega \to \omega_p$. Naturally, this is not featured by expression (4.10) obtained for the model of an infinitely thin plasma. One can adjust the expression for α_p in such a way that the dispersion law for the plasma wave will hold qualitatively for both low and high frequencies: it is sufficient to make the replacement $\alpha_p \to \alpha_p(1 - \omega^2/\omega_p^2)$. This replacement can be conjectured by considering waves in the waveguide completely filled with plasma. Equation (4.8) with this correction can be successfully employed not only in the low frequency range, but also at frequencies close to the plasma frequency.

Equation $\delta_p = 0$ describes, as follows from Eqn (4.7), the condition of exact single-particle Cherenkov resonance (wave–particle resonance). In other words, this equation defines the frequency at which the velocity of the beam is exactly the same as the phase velocity of the plasma wave. Referring to Fig. 1, it is the frequency of point *I* on the dispersion curve of the plasma wave.

Equation $\delta_p = \delta_b^-$ describes the condition of collective Cherenkov resonance (wave–wave resonance) and defines the frequency at which the phase velocities of the plasma wave and the slow beam wave are exactly the same. Referring once again to Fig. 1, it is the frequency of point *II* on the dispersion curves. The frequency of collective resonance is somewhat higher than the frequency of single-particle resonance.

Depending on the parameters of the beam-plasma system, amplification is possible in different frequency ranges. If, for instance, the coupling coefficient Θ is large, waves will be amplified over a broad frequency range, from practically zero to a frequency above the resonance frequency of point *II*. Such broad-band amplifiers have become known as Compton amplifiers. The dispersion curves of a Compton amplifier are shown in Fig. 2. These curves are calculated for the parameters of a real system: beam current — 2 kA; mean radius of the beam — 0.65 cm; beam thickness — 0.1 cm; a relativistic factor of 2; mean radius and thickness of plasma — as those of the beam; and plasma frequency — 35×10^{10} rad s^{-1}. We see that the amplification bandwidth extends from 0 to about 21×10^{10} rad s^{-1}. One may say that Fig. 2 shows what happens to Fig. 1 when the strong interaction ($\Theta = 1$) between the beam and the plasma is switched on.

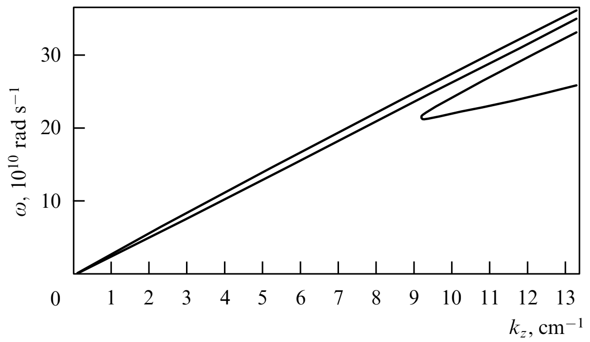

Figure 2. Dispersion curves for Compton amplifier (strong interaction between plasma and beam).

The situation is different when the coupling coefficient is small: then amplification takes place in a narrow or even very narrow band. Such narrow-band amplifiers are referred to as Raman amplifiers†. Figure 3 shows the dispersion curves plotted for the same parameters as those used in Fig. 2, the only difference being that the mean radius of the plasma tube is increased to 1.1 cm. This seemingly small separation of the plasma from the beam has considerably reduced the coupling coefficient, which has a dramatic effect on the amplification regime. The frequency band narrows down approximately from 10×10^{10} to 17×10^{10} rad s^{-1}; and the frequency of the wave–wave resonance lies somewhere within this range. Figure 3 shows what happens to Fig. 1 when the weak interaction ($\Theta \ll 1$) between the beam and the plasma is switched on.

Now let us look at the frequency dependence of the dimensionless gain δ [the proper gain is represented by the imaginary parts of k_z — that is, $\mathrm{Im}((\omega/u)\delta)$]. Although the dispersion equation (4.8) can be solved analytically (Cardano formulas), the general solutions are cumbersome and imper-

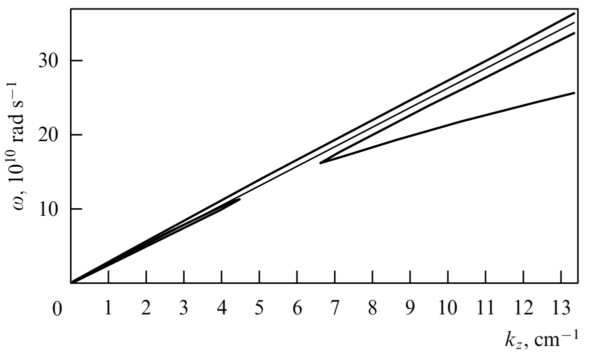

Figure 3. Dispersion curves for Raman amplifier (weak interaction between plasma and beam).

† In this context the attributes 'Compton' and 'Raman' are synonymous to 'single-particle' and 'collective'.

spicuous. Accordingly, here we shall only quote the analytical expressions for the limits of small and very high current.

When the beam current is low, and $\Theta \approx 1$, the approximate expression for the complex gain coefficient of a Compton amplifier is (in analytical expressions we retain both the imaginary and the real parts of δ; the real part of δ will be used later on for evaluating the efficiency of amplification):

$$\delta = \frac{1 - \mathrm{i}\sqrt{3}}{2} \left(\frac{1}{2\gamma^2} \, \Theta \alpha_{\mathrm{b}} \right)^{1/3} . \tag{4.12}$$

The gain (4.12) is caused by the resonant wave–particle interaction, or the stimulated emission associated with the single-particle Cherenkov effect (the term 'Compton effect' is also used by some authors [4, 34], hence the Compton amplifier). Amplification with this gain (4.12) occurs at the frequencies of both single-particle and collective Cherenkov resonances: there is no difference between these resonances in the case of low current and $\Theta \approx 1$.

If the beam current is low but $\Theta \ll 1$, the expression for the complex gain coefficient of Raman amplifier follows from Eqn (4.8):

$$\delta = \sqrt{\alpha_{\mathrm{b}}} - \mathrm{i} \left(\frac{1}{4\gamma^2} \, \Theta \sqrt{\alpha_{\mathrm{b}}} \right)^{1/2} . \tag{4.13}$$

The gain (4.13) is caused by the resonant wave–wave interaction, or the stimulated emission associated with the collective Cherenkov effect (the term 'Raman effect' is also used by some authors [4, 34], hence the Raman amplifier). Amplification with gain (4.13) only occurs at the frequency of collective Cherenkov resonance: at $\Theta \ll 1$ there is no amplification at all at the frequency of single-particle resonance.

There is a parameter which divides the single-particle and the collective effect in case of low beam currents:

$$\zeta = \frac{\Theta}{2\gamma^2 \sqrt{\alpha_{\mathrm{b}}}} = \frac{\Theta \alpha_{\mathrm{p}}}{|\alpha_{\mathrm{p}} - 1|} . \tag{4.14}$$

Formula (4.14) is written with due account for Eqns (4.10) and (4.11), the condition of wave resonance, and under the assumption that the beam current is small. Amplification with the gain (4.13) is realized when $\zeta \ll 1$, which is obviously only possible when the coupling coefficient is small. Otherwise the gain is defined by Eqn (4.12). What the beam currents are that may be regarded as small will be discussed below.

As the current increases, formulas (4.12)–(4.14) are no longer valid, and the analytical solutions of Eqn (4.8) are rather cumbersome. In this current range the results of numerical calculations are more convenient and reliable. The experimental setups discussed in this paper operate in this range of currents. Let us now embark upon discussing them.

Figure 4 shows the gain curve for a system with the same parameters as in Fig. 2 — that is, for a large coupling coefficient (curve *a*). Such a dependence is rather typical for a Compton amplifier with high beam current (Fig. 4 and similar plots only present the quantity $\mathrm{Im}\big((\omega/u)\delta\big)$ — that is, the proper gain coefficient). Two vertical straight lines in Fig. 4 mark the frequencies of the single-particle Cherenkov resonance 11.2×10^{10} rad s^{-1} (line *1*) and the collective resonance 15.1×10^{10} rad s^{-1} (line *2*). We see that the gain reaches its maximum at a frequency higher than the frequency

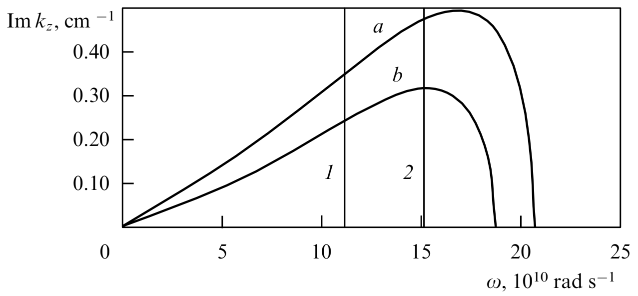

Figure 4. Gain vs. frequency for a Compton amplifier: $r_{\mathrm{p}} = 0.65$ cm (curve *a*); $r_{\mathrm{p}} = 0.8$ cm (curve *b*).

of single-particle or even collective resonance. This is a consequence of the high beam current and the associated phenomenon of aperiodical modulation of the beam in plasma which has a negative dielectric permittivity [10, 18–21]. Also, in the case of a high current the frequencies of single-particle and collective resonances are far removed from each other, but do not stand out as 'resonance' frequencies as far as the magnitude of the gain is concerned. Accordingly, one might expect the bandwidth of Compton plasma microwave amplifiers using high-current beams to be the broadest, which is indeed confirmed by the experiments [41, 42].

Figure 5 shows the frequency dependence of the gain for the case corresponding to Fig. 3 — that is, for a low coupling coefficient (the physical parameters of beam–plasma systems in Fig. 5 and Fig. 3 are the same). The dependence shown in this diagram is quite typical of Raman amplifiers. We see that the maximum gain corresponds exactly to the wave–wave resonance frequency. Moreover, there is no amplification at all at the wave–particle resonance frequency. Accordingly, the bandwidth of the Raman microwave amplifier should be narrower than that of the Compton amplifier. So far this conclusion has been only partly confirmed by experiment.

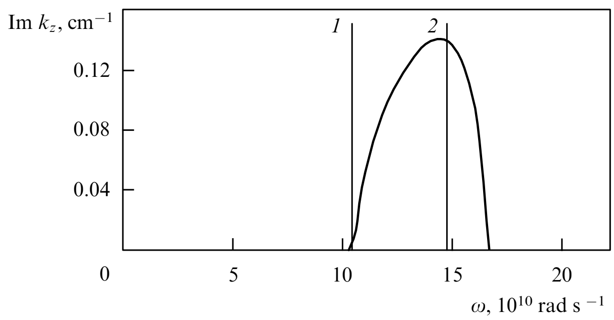

Figure 5. Gain vs. frequency for a Raman amplifier.

Observe that in any case, whether the coupling coefficient is large or small, one should anticipate a broadening of the band of amplified frequencies as the beam current increases. By way of example, let us look at the possibility of amplification of multiple waves with different azimuthal wave numbers in the experimental system under consideration. The spectra of waves in a circular waveguide containing infinitely thin plasma are given by formulas (3.3) and (3.4). Equation (3.4) includes the azimuthal wave number $l = 0, 1, 2, \ldots$ Each azimuthal wave number corresponds to a particular plasma surface wave. So far we have been considering just one of these. For instance, the results of calculations represented in the diagrams were obtained for $l = 0$. Now the question is the role of the other waves. If the beam current is small (or, more precisely, tends to zero), the answer is found from relations of the type of Eqn (3.8). At

$$\omega_{\mathrm{p}}^2 < u^2\gamma^2 k_{\perp\mathrm{p}}^2(l=0)_{\omega\to 0} \tag{4.15}$$

none of the waves is amplified. At

$$u^2\gamma^2 k_{\perp\mathrm{p}}^2(l=0)_{\omega\to 0} < \omega_{\mathrm{p}}^2 < u^2\gamma^2 k_{\perp\mathrm{p}}^2(l=1)_{\omega\to 0} \tag{4.16}$$

the azimuthally symmetrical wave is amplified, while the rest are not, and so on [equations (4.15) and (4.16) explicitly include the wave numbers (3.6)]. For a finite, and especially for a high beam current the rules of selection of modes formulated in Eqn (4.15) and (4.16) do not apply: several azimuthal modes are found under approximately the same conditions. By way of an example, Fig. 6 shows the frequency dependence of the gain in a Raman amplifier for azimuthal modes from number zero to number three. The parameters in Fig. 6 are the same as in Fig. 3 and Fig. 5. We see that the band of amplified frequencies is considerably broader than when only the azimuthally symmetrical mode is taken into account.

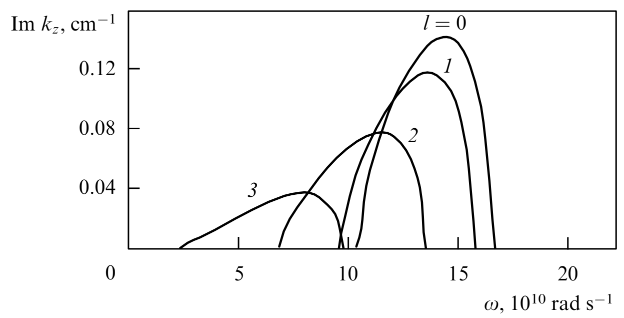

Figure 6. Gain factors for modes with azimuthal numbers $l = 0, 1, 2, 3$ for a Raman amplifier.

There is yet another mechanism of broadening of the band of amplified frequencies in case of high currents, which is associated with the finite thickness of the beam. In addition to the surface wave, a finite-thickness beam carries new waves confined in the bulk. These new waves may give rise to additional resonances — or, ultimately, to broadening of the bandwidth†. This effect may be important in the regime of the collective Cherenkov effect ($\Theta \ll 1$), when the band of amplified frequencies is narrow. Such an effect can only be revealed by numerically solving the relevant dispersion equation [66]. Let us consider it for a circular waveguide with a annular beam and a plasma whose density profiles are given by

$$P_\alpha(r) = \begin{cases} 0\,, & r < r_\alpha - \dfrac{\Delta_\alpha}{2}\,, \\ 1\,, & r_\alpha - \dfrac{\Delta_\alpha}{2} < r < r_\alpha + \dfrac{\Delta_\alpha}{2}\,, \\ 0\,, & r > r_\alpha + \dfrac{\Delta_\alpha}{2}\,, \end{cases} \tag{4.17}$$

† The finite thickness of the plasma gives rise to new plasma waves, but these waves are not excited by the relativistic beam, and so there are no additional plasma-related resonances.

where $\alpha = \mathrm{p, b}$. When $\Delta_\alpha \ll R$ the plasma and the beam are thin but not infinitesimally so [in the model of an infinitely thin beam and plasma we assumed that $P_\alpha = \Delta_\alpha \delta(r - r_\alpha)$]. The dispersion equation for profiles (4.17) is extremely unwieldy [66], and is therefore not reproduced here. Similar dispersion equations with a detailed derivation can be found, for example, in Refs [10, 55].

The results of a numerical calculation of the relevant dispersion equation are shown in Fig. 7, where the imaginary parts of the complex gain are plotted for a number of plasma frequencies. Other parameters of the system are the same as in Fig. 5. We see that at low plasma frequencies, when the amplified frequencies are not yet high and the coupling coefficient is not small, the gain behaves in the same way as in case of the single-particle Cherenkov effect, and there is nothing peculiar about it. When, however, the plasma frequency is 35×10^{10} rad s^{-1}, the gain behaves as in case of the collective Cherenkov effect, and we observe a new feature: in addition to the amplification in the main frequency band (the gain represented in Fig. 5 for the model of an infinitely thin beam and plasma) there is amplification in another band marked on the diagram with vertical dashed lines. This band is attributed to the interaction of the bulk beam wave with the surface plasma wave. This interaction is not as efficient as the interaction between the surface beam and plasma waves. It can be demonstrated that the ratio of the respective gains is of the order of $(\Delta_{\mathrm{b}}/R)^{1/4}$. This estimate follows from Eqn (4.13) and the estimated transverse wave numbers of the bulk and the surface waves. Note that experiments [41, 42] indicate that the transverse profiles of the beam and the plasma are much more sophisticated than the profile described by Eqn (4.17). Therefore, the issue of the possible mechanisms of additional broadening of the amplified frequency band cannot be regarded as completely resolved.

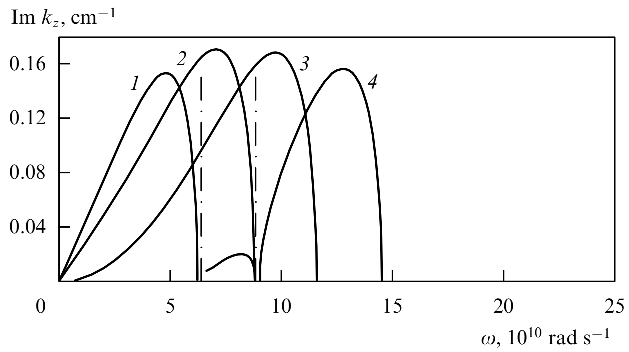

Figure 7. Gain factors for azimuthally symmetrical modes in the model of a finite-thickness tubular beam and plasma: $\omega_{\mathrm{p}} = 20 \times 10^{10}$ rad s^{-1} (curve *1*); $\omega_{\mathrm{p}} = 25 \times 10^{10}$ rad s^{-1} (curve *2*); $\omega_{\mathrm{p}} = 30 \times 10^{10}$ rad s^{-1} (curve *3*); $\omega_{\mathrm{p}} = 35 \times 10^{10}$ rad s^{-1} (curve *4*).

As the electron beam current further increases into the region not yet covered by experimental studies, Eqn (4.8) again admits a simple analytical solution.

When, for example, the current is very large†, at the frequency of single-particle Cherenkov resonance, when

† Later on we shall define the concept of a large current. Here we just indicate that a 'very large current' implies that $|2\gamma^2\delta| \gg 1$.

$\delta_p = 0$, Eqn (4.11) reduces to the form

$$\delta^3 = -\frac{\Theta\alpha_b}{2\gamma^2}(1 + 2\gamma^2\delta)\left(1 - 2\gamma^2\delta\,\frac{1-\Theta}{\Theta}\right). \tag{4.18}$$

It is easy to see that when the coupling coefficient Θ is small, Eqn (4.18) has no complex roots, which means that there is no amplification. Recall that the same occurs at the frequency of the exact Cherenkov resonance at $\Theta \ll 1$ when the beam current is not that large. At $\Theta \approx 1$, however, Eqn (4.18) reduces to

$$\delta(\delta^2 + \alpha_b) = -\frac{\alpha_b}{2\gamma^2}\,. \tag{4.19}$$

Equation (4.19) describes two coupled oscillatory systems: a stable plasma system with $\delta = 0$ (no amplification), and an aperiodically unstable beam system with

$$\delta = -\mathrm{i}\sqrt{\alpha_b}\,. \tag{4.20}$$

The gain (4.20) is due not to the excitation of plasma waves by the beam, but rather by the aperiodical modulation of the beam in a plasma whose permittivity is negative [18, 19, 21]. A similar process in the low-current beam and with $\Theta \approx 1$ is only possible at frequencies much below the frequency of the single-particle Cherenkov resonance. When the beam current is very large, the amplification becomes aperiodical even at the single-particle resonance frequency.

Consider now amplification at the collective resonance frequency in the case of high currents. When the current is high, the spectrum of the slow beam wave changes. From the general expression (4.11) it follows that

$$\delta_b^- \approx 2\gamma^2\alpha_b\,. \tag{4.21}$$

The wave with spectrum (4.21) is highly non-potential. Accordingly, it is more like a wave of current density than a wave of charge density. Now taking into account the condition $\delta_p = \delta_b^-$ of collective wave–wave resonance, from Eqn (4.8) we get the expression

$$\delta = \gamma^2\alpha_b(2 - \Theta) - 2\mathrm{i}\gamma^2\alpha_b\sqrt{\Theta - \frac{\Theta^2}{4}} \tag{4.22}$$

for the gain which holds for arbitrary Θ. When the coupling coefficient is small the imaginary part of Eqn (4.22) defines the gain due to the relativistic collective Cherenkov effect. When, however, the coupling coefficient is close to one, Eqn (4.22) becomes

$$\delta = (1 - \mathrm{i}\sqrt{3})\gamma^2\alpha_b\,. \tag{4.23}$$

The gain (4.23) is due both to the relativistic collective Cherenkov effect and to the effect of self-modulation of the beam in a medium with negative permittivity.

5. Generation

So far we have been mainly concerned with the amplification of plasma waves by an electron beam. Now we are going to deal with generation. The amplified wave is partially reflected from the boundary $Z = L$ of the plasma waveguide and returns some of the energy received from the beam back into the system. This may cause self-excitation of the amplifier — that is, the onset of generation. Obviously, generation is not a welcome phenomenon for designers of amplifiers. Therefore, an important task of the theory is to define the conditions of the onset of generation.

We use the following notation: A_0 is the amplitude of the wave from external source at the input boundary $Z = 0$; A^+ is the amplitude of the wave amplified by the beam at $Z = 0$; A^- is the amplitude of the plasma wave traveling backwards and acting as the feedback; $\varkappa$ is the coefficient of reflection of the amplified wave from the boundary $Z = L$; δ^+ is the gain factor for the plasma wave [the modulus of the imaginary part of the quantity (4.7), plotted in Figs 4–7].

At the boundary $Z = L$ the amplitude of the amplified wave is $A^+\exp(\delta^+L)$. At the same boundary, the amplitude of the backward wave is given by

$$A^- = A^+\varkappa\exp(\delta^+L)\,. \tag{5.1}$$

Since the backward wave does not interact with the beam, the same expression defines the amplitude of the backward wave at $Z = 0$. In addition, at $Z = 0$ the amplitudes of the input, backward and amplified waves balance out:

$$A^+ = A^- + A_0\,. \tag{5.2}$$

The expression for the amplitude of the amplified wave follows from Eqns (5.1) and (5.2):

$$A^+ = \frac{A_0}{1 - \varkappa\exp(\delta^+L)}\,. \tag{5.3}$$

Self-excitation of a plasma amplifier occurs when the amplitude of an amplified wave goes to infinity. Hence follows the condition of the onset of generation:

$$\delta^+ = \frac{1}{L}\ln(4\gamma^2)\,. \tag{5.4}$$

In writing (5.4) we used the estimate

$$\varkappa = \frac{1}{4\gamma^2} \tag{5.5}$$

for the coefficient of reflection proposed in Refs [61, 42] and refined in Ref. [45]. This estimate holds for a cable plasma wave emitted into a coaxial horn in a sufficiently low-frequency range.

Of course, our derivation of Eqn (5.4) is not rigorous, but the result is nevertheless reasonably correct. More precisely, the factor of four under the logarithm in Eqn (5.4) ought to be replaced by ten [2, 10].

It will be worthwhile to get order-of-magnitude estimates for a real plasma-beam system. Assume that the relativistic factor of the beam is, as before, equal to 2, and the length of the system L varies from 10 to 30 cm. Under these assumptions the magnitude (5.4) of the 'threshold' gain varies from about 0.1 to 0.3 cm^{-1}. By order of magnitude this is exactly the same as what was calculated from the dispersion equation (4.8) for the experimental beam and plotted in Figs 4–7. This estimate is supported by the next diagram.

The isolines for the gain for the zeroth azimuthal mode are plotted in Fig. 8 in coordinates of plasma radius versus plasma frequency. The isolines are plotted from the numerical solution of the dispersion equation (4.8). The values

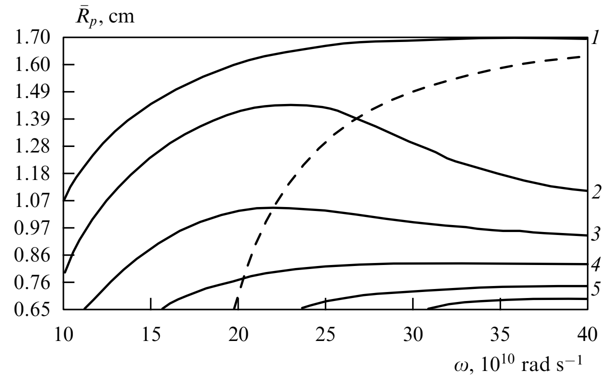

Figure 8. Isolines of gain: $\delta^+ = 0$ (curve *1*); $\delta^+ = 0.1$ (curve *2*); $\delta^+ = 0.2$ (curve *3*); $\delta^+ = 0.3$ (curve *4*); $\delta^+ = 0.4$ (curve *5*). Dashed line indicates the plasma frequency threshold for the symmetrical mode. Beam current $I_b = 2$ kA.

found from Eqn (5.4) are of the same order of magnitude as those represented by the isolines. It follows that the experiments of Refs [6, 35–37, 41, 42], to which we are referring here, were carried out in circumstances where it was hard to establish whether the system operated as an amplifier or as a generator. In all likelihood, it was an amplifier in Ref. [41], and a generator in Ref. [42].

Figure 8 also indicates the threshold (dashed line), calculated according to Eqn (3.8) for the symmetrical mode. We see that for a current of 2 kA, the amplification starts at plasma frequencies much lower than defined by Eqn (3.8). This fits in well with the results of recent experiments [42], in which the threshold plasma density above which the emission starts was measured.

6. Efficiency of a plasma microwave amplifier

Going over from the linear treatment to the problems of nonlinear theory, we begin with the efficiency of amplification of plasma waves by a relativistic electron beam. There is a very important parameter which defines not only the regime of amplification of waves in a plasma, but also the efficiency of a plasma microwave amplifier. Let us introduce this parameter from the standpoint of efficiency.

The efficiency can obviously be defined as $E = \langle \Delta\gamma/(\gamma-1) \rangle$, where $\Delta\gamma$ is the change in the relativistic factor of an individual electron of the beam, and the angular brackets denote averaging over all electrons of the beam which have been engaged in the resonant interaction with the plasma wave. Expressing the change $\Delta\gamma$ via the change Δu in the velocity of an electron of the beam, we may rewrite the formula for the efficiency as

$$E = \gamma(\gamma+1)\left\langle \frac{\Delta u}{u} \right\rangle \approx \gamma^2 \left\langle \frac{\Delta u}{u} \right\rangle .$$

To get an estimate for the maximum change Δu in the velocity, we note that this change is not greater than the difference between the unperturbed beam velocity u and the phase velocity of the amplified wave. Recall that the amplified wave always lags behind the electron beam, which is evident from Eqn (4.7) and formulas (4.12), (4.13), (4.22) and (4.23). Making use of Eqn (4.7), we may write

$$E \approx \gamma^2 \operatorname{Re}(\delta) \approx \gamma^2 |\delta| ,$$

where δ is found from Eqn (4.8). Obviously, our estimate is correct if the resulting value of E is much less than unity. The main thing, however, is that the efficiency of amplification is determined by the parameter $2\gamma^2|\delta|$ †. The value of δ to be used in this expression depends on the operating regime of the amplifier. Let us begin with the Compton amplifier, when Θ is close to one.

Substituting (at $\Theta = 1$) the single-particle gain factor (4.12) into $2\gamma^2|\delta|$, and making use of the second relation in Eqn (4.9), we get the following expression for the efficiency parameter:

$$\mu_1 = \left(4\,\frac{\omega_b^2 \gamma^{-1}}{k_{\perp b}^2 u^2} \right)^{1/3} . \tag{6.1a}$$

Expressing the Langmuir frequency of the electron beam in terms of the beam current, and making use of the expression for $k_{\perp b}^2$, we finally find the efficiency parameter for a Compton amplifier:

$$\mu_1 = \left(\frac{I_b}{2\gamma} \ln \frac{R}{r_b} \right)^{1/3} . \tag{6.1b}$$

Here I_b is the electron beam current in kiloAmperes. When the relativistic parameter γ is large, the parameter (6.1b) is proportional to the cube root of the ratio of the beam current to the limiting vacuum current [1, 9, 29]; because of this it is sometimes referred to as the high-current parameter.

So, if parameter (6.1b) is small, the efficiency of amplification E is directly proportional to this parameter. A more general result also holds [4, 8, 10]:

$$E \approx \begin{cases} \mu_1 , & \mu_1 \ll 1 , \\ \mu_1^{-3} , & \mu_1 \gg 1 . \end{cases} \tag{6.2}$$

According to numerical calculations, the maximum efficiency is realized at $\mu_1 \approx 1$ and may be as high as 20% (assuming, of course, that the length of amplifier is selected properly, of which we shall speak later).

Now we can define the concepts of low current, large current, and very large current. When $\mu_1 \ll 1$, the beam current must be regarded as low. It is for such low currents that formula (4.12) for the complex gain holds. Conversely, when $\mu_1 \gg 1$, the beam current is very high. Equations (4.20)–(4.23) apply to such currents. When, however, $\mu_1 \approx 1$, the beam current is simply high — it is of the order of the limiting vacuum current. It is currents of this magnitude that are realized in modern experiments in plasma microwave electronics. A little later we shall explain why it is so.

Now let us consider the efficiency of the Raman amplifier. Substituting the value of Eqn (4.13) into the parameter $2\gamma^2|\delta|$, and noting that $\Theta \ll 1$, we find that

$$\mu_2 = \left(4\,\frac{\omega_b^2 \gamma^{-1}}{k_{\perp b}^2 u^2} \right)^{1/2} = \mu_1^{3/2} . \tag{6.3}$$

Actually, for the Raman amplifier we have the same parameter as in the case of the Compton amplifier, only the

† The factor of two appears here not only because of tradition, but also because the same parameter enters the dispersion equation (4.8) and is definitive for the character of its solutions. For example, formulas (4.12) and (4.13) only hold when $2\gamma^2|\delta| \ll 1$.

exponent is different. The concepts of small, high, and very high currents are still valid. For example, formula (4.13) only holds in the limit of low current, when $\mu_2 \ll 1$. There is also an estimate for the efficiency of a Raman amplifier similar to Eqn (6.2) [4, 8, 10]:

$$E \approx \begin{cases} \mu_2 , & \mu_2 \ll 1 , \\ \mu_2^{-1} , & \mu_2 \gg 1 . \end{cases} \tag{6.4}$$

The maximum efficiency (which is somewhat less than that of the Compton amplifier) again corresponds to $\mu_2 \approx 1$.

It turns out that the experimental systems currently studied in plasma microwave electronics operate in conditions close to optimal in terms of the efficiency of amplification. The point is that the experiments we are referring to employ the high-current electron beam accelerators using diodes with magnetic insulation.

Let us use the dependence between the current in the high-current beam and the relativistic factor of the beam in the diode with magnetic insulation [64, 65]:

$$I_{\rm b} = \frac{G}{\ln(R/r_{\rm b})} \frac{(\gamma - 1)^2}{(\gamma^{2/3} + 2)(\gamma^{2/3} - 1)^{1/2}} . \tag{6.5}$$

The numerical coefficient G in Eqn (6.5) can be selected on the basis of experimental data [42], especially the most recent measurements [67] of the current in the electrodynamic system of the amplifier as a function of the accelerating voltage in the diode — that is, of the relativistic factor γ. From experiment we have $G \approx 5.5$. Further substituting Eqn (6.5) into Eqn (6.1b), we find the dependence of the large-current parameter μ_1 on the relativistic factor, represented in Fig. 9. For $\gamma \to \infty$ we have $\mu_1 \to (G/2)^{1/3} \approx 1.4$, and for the values of the relativistic factor realized experimentally (a few units and more) the parameter (6.1b) [like (6.3) for that matter] is close to unity, and therefore the amplification regime is close to optimal. One must bear in mind that optimal efficiency can only be attained through optimizing the length of the amplifier and the frequency of the amplified signal, which will be discussed later within the framework of nonlinear theory. There are two more issues, however, that call for our attention.

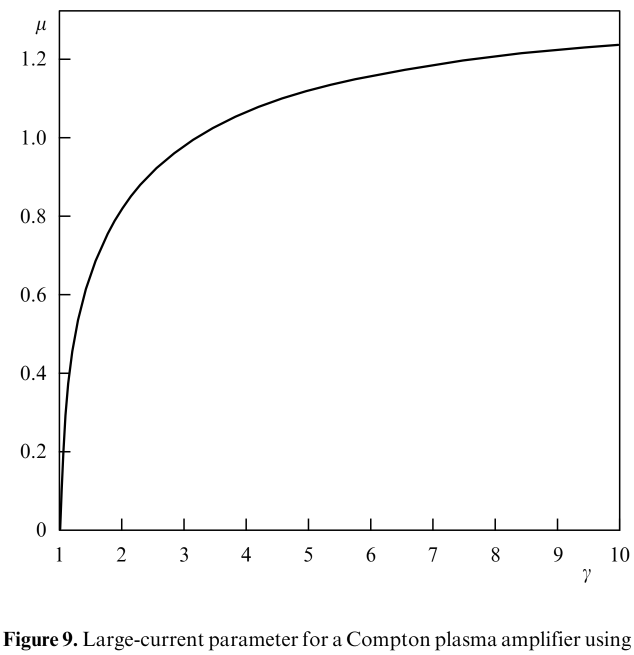

Figure 9. Large-current parameter for a Compton plasma amplifier using a magnetic insulation diode vs. relativistic factor of the electron beam.

On the strength of the above definition of the efficiency of amplification we may write the formula

$$W = 511(\gamma - 1) E I_{\rm b} \tag{6.6}$$

for the output power of the amplifier, where the beam current is in kiloamperes. For the experimental parameters ($\gamma = 2$, $I_{\rm b} = 2$ kA) we have $W \approx 1000E$ MW. In experiments (see, for example, Refs [6, 42, 67] the output power was reported to be 200 MW and more, which agrees perfectly with the efficiency predicted by the theory. Also reported were much less impressive experimental results. They are most likely explained by poor optimization of the system length.

One final remark: the estimates obtained in this section are based on the most general physical considerations. They hold for any amplifier irrespective of its construction, which will only determine the particular form of the parameter (6.1b). In the case of a cyclotron resonance maser, for example, it will involve the transverse velocity of electrons of the beam, the depth of corrugation in the case of an amplifier with a bellows-shaped resonator, the amplitude of the alternating field in the case of an undulator, etc. In this respect the plasma microwave amplifier is unique, since parameter (6.1b), which determines its efficiency and operating regime, is very simple in structure, and is close to unity for the currents realized in all high-current relativistic microwave sources, including vacuum sources. At the same time, the physically similar parameter for vacuum systems may have a quite different value. Besides, the working current in a plasma system can be made much larger than in any vacuum system†, which permits a considerable increase of the output power (6.6).

7. Nonlinear equations for a plasma amplifier

In our presentation of the nonlinear theory we start with the general nonlinear equations (2.1)–(2.6), which will be converted into a form convenient for solving the problem of amplification of waves. The following circumstances must be taken into account: firstly, the transverse structure of the wave field in the plasma-beam waveguide is not known in advance, but rather is established in a self-consistent way as progress is made towards larger values of Z; secondly, the frequency spectrum of the amplified signal is not necessarily specified, which makes it necessary to consider the simultaneous amplification of waves having different frequencies; thirdly, the longitudinal wave numbers of all waves amplified by the beam are close to the frequency of the wave divided by the unperturbed velocity of the beam. These considerations suggest the following representation of the polarization potential of the field in the problem of wave amplification:

$$\psi = \frac{1}{2} \sum_{n=1}^{\infty} \left\{ \varphi_n(\mathbf{r}_\perp) \times \sum_{s=1} \left[A_{ns}(z) \exp\left(-\mathrm{i}s\Omega t + \mathrm{i}s \frac{\Omega}{u} z \right) + \text{c.c.} \right] \right\} . \tag{7.1}$$

† When $r_{\rm p} > r_{\rm b}$, the current may be increased by a factor of $\ln(R/r_{\rm b})/\ln(r_{\rm p}/r_{\rm b})$.

Here Ω is a certain low frequency used for 'discretization' of the spectrum of the amplified signal. Summation over n in Eqn (7.1) determines the transverse structure of the field, and summation over s determines the frequency spectrum.

Observe that the 'discretization' of the spectrum and the introduction of the small frequency Ω have a simple physical meaning. As a matter of fact, the field in any cross section of the waveguide Z can be represented as a Fourier integral with respect to frequency ω. The approximate calculation of this integral is facilitated by transition to a summation with a discrete step $\omega_s = s\Omega$, $s = 1, 2, \ldots$ This procedure is reflected in Eqn (7.1). The selection of the small frequency Ω is dictated either by the desired accuracy of representation of the spectrum, or by physical considerations. If, for example, the duration of the pulse is T, it would be natural to set $\Omega = 2\pi/T$.

Our next task consists in constructing the equations for the amplitudes $A_{ns}(z)$ (or, more precisely, certain equivalent quantities, as will presently become clear). Note that the introduction of amplitudes is only justified if they change more slowly than $\exp\left[\mathrm{i}s(\Omega/u)z\right]$ — that is, if the amplification of the field on the scale of one wavelength is small. We assume that the amplitudes change slowly, which in the language of the linear approximation [see Eqn (4.7)] is equivalent to the condition $\delta \ll 1$, which holds for the beams currently used. That this condition is satisfied in our situation is clear from Figs 4–6.

Let us briefly run through the main steps in the construction of the nonlinear equations for a microwave amplifier with a thin electron beam and plasma. Using the first expression in Eqn (2.2), Eqn (2.3), and relations (2.4) and (7.1), we represent the function j_{p} in the form

$$j_{\mathrm{p}} = \frac{1}{2}\sum_{s=1}\left[\tilde{j}_{\mathrm{p}s}(\mathbf{r}_\perp, z)\exp\left(-\mathrm{i}s\Omega t + \mathrm{i}s\,\frac{\Omega}{u}\,z\right) + \text{c.c.}\right]. \tag{7.2}$$

It is not necessary to expand the functions $\tilde{j}_{\mathrm{p}s}(\mathbf{r}_\perp, z)$ in the eigenfunctions of the waveguide. Substituting now Eqn (7.1), (7.2) and (2.5) into Eqns (2.1), (2.3) and (2.4), and taking into account the orthogonality of the functions $\varphi_n(\mathbf{r}_\perp)$ and $\exp\left[\mathrm{i}s(\Omega/u)z\right]$, we get the following intermediate results:

$$E_z = \frac{1}{2}\sum_{n=1}^{\infty}\left\{\varphi_n(\mathbf{r}_\perp)\right.$$
$$\left.\times\sum_{s=1}\left[\widehat{A}_{ns}(z)\exp\left(-\mathrm{i}s\Omega t + \mathrm{i}s\,\frac{\Omega}{u}\,z\right) + \text{c.c.}\right]\right\},$$
$$\widehat{A}_{ns}(z) = -s^2\,\frac{\Omega^2}{u^2\gamma^2}\left(1 - \mathrm{i}2\gamma^2\,\frac{u}{s\Omega}\,\frac{\mathrm{d}}{\mathrm{d}z}\right)A_{ns}(z)\,, \tag{7.3a}$$

$$-\,\mathrm{i}s\Omega\,\tilde{j}_{\mathrm{p}s}(\mathbf{r}_\perp, z) = \frac{\omega_{\mathrm{p}}^2}{4\pi}\sum_{n=1}^{\infty}\varphi_n(\mathbf{r}_\perp)\widehat{A}_{ns}(z)\,,$$
$$\mathrm{i}s\Omega\|\varphi_n\|^2\left[k_{\perp n}^2 + s^2\,\frac{\Omega^2}{u^2\gamma^2}\left(1 - \mathrm{i}2\gamma^2\,\frac{u}{s\Omega}\,\frac{\mathrm{d}}{\mathrm{d}z}\right)\right]A_{ns}$$
$$= -4\pi S_{\mathrm{p}}\varphi_n(\mathbf{r}_{\mathrm{p}})\tilde{j}_{\mathrm{p}s}(\mathbf{r}_{\mathrm{p}}, z) - 4\pi S_{\mathrm{b}}\varphi_n(\mathbf{r}_{\mathrm{b}})\langle j_{\mathrm{b}}\rangle_s\,,$$
$$\langle j_{\mathrm{b}}\rangle_s = \frac{\Omega}{\pi}\int_0^{2\pi/\Omega} j_{\mathrm{b}}\exp\left(\mathrm{i}s\Omega t - \mathrm{i}s\,\frac{\Omega}{u}\,z\right)\mathrm{d}t\,. \tag{7.3b}$$

Here j_{b} is the beam current (2.5). The second expression in Eqn (7.3b) involves the functions $\tilde{j}_{\mathrm{p}s}$ only at the point where the plasma is — that is, at only one point in the transverse cross section of the waveguide. This circumstance, which is characteristic for the case of a thin plasma, makes our job much simpler. We denote the amplitudes of the sth harmonics in the plasma and the beam by $j_s \equiv \tilde{j}_{\mathrm{p}s}(\mathbf{r}_{\mathrm{p}})$ and $\langle j_{\mathrm{b}}\rangle_s \equiv en_{\mathrm{b}}u\rho_s$ respectively, and the amplitude of the sth harmonic of perturbation of the beam density by ρ_s. The latter quantity is made dimensionless by normalizing it to n_{b}. It is convenient to reformulate equations (7.3) in terms of only the z-dependent variables j_s and ρ_s. First we transform the expressions for the amplitudes of the harmonics of the beam current. Making use of Eqn (2.5), we replace the integration over t in Eqn (7.3b) with integration over t_0. Then we introduce the new variables

$$y = \Omega\left[t(z, t_0) - \frac{z}{u}\right], \qquad y_0 = \Omega t_0\,,$$
$$\eta = \frac{u - v(z, t_0)}{v(z, t_0)}\,, \qquad \xi = \frac{\Omega}{u}\,z\,, \tag{7.4}$$

where $t(z, t_0)$, $v(z, t_0)$ are the solutions of the set of characteristic equations (2.6). Using the first three variables from Eqn (7.4), we get:

$$\rho_s = \frac{1}{\pi}\int_0^{2\pi}(1+\eta)^{-1}\exp(\mathrm{i}sy)\,\mathrm{d}y_0 \approx \frac{1}{\pi}\int_0^{2\pi}\exp(\mathrm{i}sy)\,\mathrm{d}y_0\,. \tag{7.5}$$

The 'approximately equals' sign in Eqn (7.5) is the consequence of the small change of the velocity of the beam electrons at all stages of amplification [it can be demonstrated that the change in the velocity is of the order of $|\delta|$ from Eqn (4.7)]. As shown in Ref. [60], the smallness of the change of the beam electrons' velocity is crucial for the validity of the initial equation (2.5) with the characteristics (2.6).

Further we proceed as follows. From the second relation in Eqn (7.3b) we express the amplitudes A_{ns}. This is especially easy in the case of sufficiently low frequencies, when the upper frequency in the spectrum of the amplified signal is small compared to $k_{\perp 1}u\gamma$, and the derivative on the left-hand side of the second relation in Eqn (7.3b) may be neglected. For the sake of simplicity we shall confine ourselves here to this most important case (the same approximation was used in the linear theory; the more general case is considered in Ref. [43]). Now the first relation in Eqn (7.3b) we multiply by $\delta(\mathbf{r}_\perp - \mathbf{r}_{\mathrm{p}})$ and integrate over the cross section of the waveguide, getting the equations in $j_s(z)$ as a result. With due account for Eqn (7.3a), we substitute the coefficients A_{ns} into these equations and Eqn (2.6), and go over to the dimensionless longitudinal coordinate ξ [see Eqn (7.4)]. Finally we come to the following set of equations:

$$\frac{\mathrm{d}y}{\mathrm{d}\xi} = \eta\,,$$
$$\frac{\mathrm{d}\eta}{\mathrm{d}\xi} = \frac{\mathrm{i}}{2}\left(1 + 2\gamma^2\,\frac{u^2}{c^2}\,\eta\right)^{3/2}$$
$$\times\sum_{s=1}\left[s\exp(-\mathrm{i}sy)\widehat{L}_s(\alpha_{\mathrm{b}s}\,\rho_s + j_s) - \text{c.c.}\right],$$
$$(1 - \alpha_{\mathrm{p}s}\widehat{L}_s)\,j_s = \Theta_s\alpha_{\mathrm{p}s}\alpha_{\mathrm{b}s}\widehat{L}_s\,\rho_s\,. \tag{7.6}$$

Here

$$\widehat{L}_s = 1 - 2\mathrm{i}\gamma^2\,\frac{1}{s}\,\frac{\mathrm{d}}{\mathrm{d}\xi}\,, \tag{7.7}$$

ρ_s is given by Eqn (7.5), and the coefficients α_{ps}, α_{bs}, Θ_s are defined by Eqns (4.5), (4.6) and (4.9) with the following replacement (the general form of the limiting formulas (4.5) and (4.6) can be found in Ref. [62]):

$$\chi^2 \to s^2 \frac{\Omega^2}{u^2\gamma^2}\,, \qquad s = 1, 2, \ldots \tag{7.8}$$

Let us also quote an alternative form of the third equation in Eqn (7.6), to make it clear that it precisely defines the amplitudes and spectra of the plasma waves:

$$\frac{\mathrm{d}j_s}{\mathrm{d}\xi} - \mathrm{i}\delta_{ps} j_s = -\frac{\mathrm{i}}{2\gamma^2}\, s\Theta_s \alpha_{bs} \widehat{L}_s \rho_s\,. \tag{7.9}$$

Here

$$\delta_{ps} = \frac{s}{2\gamma^2}\left(\frac{1}{\alpha_{ps}} - 1\right) \tag{7.10}$$

is the counterpart of the quantity (4.10).

As indicated above, equations (7.6) were derived in the low-frequency limit. They can be easily generalized to higher frequencies [10, 43]. To do this on a qualitative level, as in the linear theory, it is sufficient to carry out the replacement

$$\alpha_{ps} \to \alpha_{ps}\left(1 - s^2 \frac{\Omega^2}{\omega_p^2}\right).$$

The dispersion equation (4.8) follows from Eqn (7.6) in the linear approximation.

The first integral of equations (7.6), which expresses the conservation of the flow of energy along the waveguide, has the form

$$\begin{aligned} \langle P\rangle &+ \frac{q\gamma^2}{4}\sum_{s=1}\Theta_s^{-1}\alpha_{bs}^{-1}|j_s|^2 + \frac{q\gamma^2}{4}\sum_{s=1}\alpha_{bs}|\rho_s|^2 \\ &+ \frac{q\gamma^2}{4}\sum_{s=1}(j_s\rho_s^* + j_s^*\rho_s) = \text{const}\,, \\ \langle P\rangle &= \frac{1}{2\pi}\int_0^{2\pi}(1+q\eta)^{-1/2}\,\mathrm{d}y_0\,. \end{aligned} \tag{7.11}$$

Here $\langle P\rangle$ is the mean flow of mechanical energy of the beam electrons related to the flow of mechanical energy of the unperturbed beam; the terms proportional to $q\gamma^2/4$ define the flows of energy of plasma and beam waves with due account for their interaction, and $q = 2\gamma^2(u/c)^2$. Some asymmetry with respect to j_s and ρ_s in Eqn (7.11) is due to the different procedures of normalization; the replacement $j_s \to \sqrt{\Theta_s\alpha_{bs}\alpha_{ps}}\,\rho_{ps}$ restores symmetry with respect to ρ_s, ρ_{ps}.

The efficiency of emission of the beam is defined as the relative part of the flow of the kinetic energy converted into the flow of energy of the waves:

$$E = 1 - \langle P\rangle\,. \tag{7.12}$$

This is the same quantity as found in Eqns (6.2), (6.4) and (6.6). Strictly speaking, Eqn (7.12) defines the part of the flow of electromagnetic energy transferred not only to the plasma wave but also to the beam wave, as is clear from Eqn (7.11). For the actual experimental parameters, however, the plasma part is definitive, which allows us to disregard these insignificant details.

Let us also consider the additional conditions imposed on Eqn (7.6) which are defined at the input boundary of the amplifier $Z = 0$. It is possible, for example, that plasma oscillations with a certain spectral distribution are excited at the input boundary, and an unperturbed electron beam is injected. This situation corresponds to the following additional conditions:

$$\begin{aligned} j_s\Big|_{\xi=0} &= j_{s0}\,, \\ y\Big|_{\xi=0} &= y_0 \in [0, 2\pi]\,, \\ \eta\Big|_{\xi=0} &= 0\,. \end{aligned} \tag{7.13}$$

Alternatively, one could imagine a different situation: no plasma waves are supplied to the input, and the density (or velocity) of the injected electron beam is modulated. In the case of density modulation, the additional conditions may have the form

$$\begin{aligned} j_s\Big|_{\xi=0} &= 0\,, \\ y\Big|_{\xi=0} &= y_0 + \frac{1}{2}\sum_{s=1}\left[b_s\exp(\mathrm{i}sy_0) + \text{c.c.}\right], \\ \eta\Big|_{\xi=0} &= 0\,, \qquad y_0 \in [0, 2\pi]\,. \end{aligned} \tag{7.14}$$

We shall use this last set of additional conditions. The quantities b_s in Eqn (7.14) define the depth of the initial modulation of the beam at the respective harmonic. The values selected for the calculations were small in magnitude (about 0.01 – 0.05), which ensured low initial modulation of the beam ($|b_s| \approx 1$ corresponds to a 100% modulation of the beam). Modulation of the form (7.14) will be referred to as regular modulation of the beam. Indeed, as will become clear from our subsequent discussion, under the conditions (7.14) the beam at $Z = 0$ appears as a homogeneous background against which compact clusters are injected into the waveguide at regular intervals of $2\pi/\Omega$. One may also consider the case of chaotic modulation of the beam. Then the second relation in Eqn (7.14) must be replaced by

$$y\Big|_{\xi=0} = y_0 + b_s q_s\,, \qquad y_0 \in [0, 2\pi]\,, \tag{7.15}$$

where q_s are random numbers from the interval $[-1, 1]$.

One last comment: it is worthwhile solving two variants of the problem (7.6) and (7.14). One corresponds to the case when the sum in the second relation in Eqn (7.14) involves a large number of terms, and the frequencies $s\Omega$ rather densely fill the frequency range from 0 to ω_p. This is the problem of a broad-band or noise amplifier. Conversely, the sum in Eqn (7.14) may contain just one term with $s = 1$. This is the problem of a narrow-band or monochromatic amplifier. Amplification of monochromatic signal has been considered in numerous publications (see, for example, Refs [4 – 10, 43]), so we are going to concentrate on broad-band amplification.

8. Spatial dynamics of amplification and the spectra of a plasma amplifier

Since the plasma frequencies in experiments did not exceed 35×10^{10} rad s^{-1}, the frequency range selected for numerical simulation of the broad-band amplifier extended from zero to

40×10^{10} rad s^{-1}. A total of $S_{\max}$ modes were evenly distributed over this interval. Equations (7.6) were solved for each s from 1 to $S_{\max}$. The number of large clusters simulating the beam was $10S_{\max}$. In different calculations $S_{\max}$ varied from 30 to 50. The following aspects are considered below: the spatial distribution (along the Z axis) of the efficiency of emission (7.12); the spatial distribution of absolute values of the amplitudes of harmonics whose frequencies are closest to the wave – particle and wave – wave resonances; and the spectral distribution of the flow of electromagnetic energy in plasma waves.

Let us start our discussion with the Compton amplifier based on the single-particle Cherenkov effect. Since the case $r_{\mathrm{p}} = r_{\mathrm{b}}$ is technically hard to realize, we set $r_{\mathrm{p}} = 0.8$ cm, the remaining parameters being the same as in Fig. 4. The gain for this case is represented on the same diagram by curve b, and the resonance frequencies are as follows: 11×10^{10} rad s^{-1} for the wave – particle resonance, and 15×10^{10} rad s^{-1} for the wave – wave resonance.

Figure 10 shows the spectra of the amplified signal close to the input of the amplifier (where Z is of the order of tenths of a centimeter). The frequency is plotted on the horizontal axis; the vertical axis shows the spectral distribution of the electromagnetic energy of plasma waves. Also marked on the diagram are the frequencies of the wave – particle (straight line *1*) and wave – wave (line *2*) resonances. The vertical dash (right above the frequency axis) indicates the upper limit of the amplification zone according to the linear theory. The insert in the upper left corner of Fig. 10 shows the phase plane of the beam electrons. Plotted on the horizontal axis of the phase plane are the flight times of all electrons which have reached the given cross section of the waveguide in the time interval from zero to $2\pi/\Omega$; the vertical axis is graduated in the perturbations of the electron velocity (in relative units).

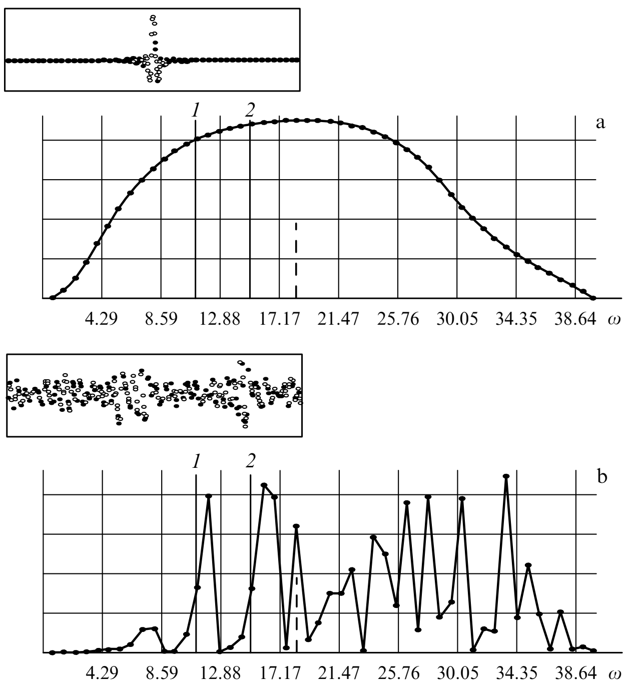

Figure 10. Spectral distribution of energy flow in plasma wave near the input cross section of Compton amplifier: (a) regular density modulation; (b) chaotic density modulation.

Let us explain whence the perturbations of the electrons' velocity arise at small Z. As follows from the last condition in Eqn (7.14), there are no perturbations at $Z = 0$. As follows from the second relation in Eqn (7.14), or from Eqn (7.15), the electrons are injected into the waveguide in bursts, and so even at $Z = 0$ there are perturbations of density, whereas $\rho_s \approx b_s$. These perturbations create an electric field which perturbs the velocity of the electrons.

Figure 10a corresponds to regular density modulation of the beam [boundary conditions (7.14)]. From the phase diagram we see that the perturbations of the electrons' velocity are local; accordingly, the field is a sequence of local wave pulses with a time spacing of $2\pi/\Omega$. The pulsed nature of the field can also be seen from the spectral density of the radiation: leaving aside the fall-offs at the high and low-frequency edges, all lines in the emission spectrum have about the same intensity. Accordingly, the shape of a single field pulse can be approximated by finding the sum of a simple geometric progression:

$$\operatorname{Re}\left(\sum_{s=1}^{S_{\max}} \exp(\mathrm{i}sy)\right) = \frac{\sin(S_{\max}y/2)}{\sin(y/2)} . \tag{8.1}$$

This formula agrees very well with the electron distribution in the phase plane. So we see that in case of regular modulation the sequence of wave pulses of the type of Eqn (8.1) excited by the beam at small values of Z is amplified. The pulses follow one after another at intervals $2\pi/\Omega$.

Figure 10b shows the case of chaotic modulation of the beam, when boundary condition (7.15) is used. From the phase diagram we see that the perturbations of the electron velocity are not localized, but rather involve the entire beam. As a consequence, the field excited by the beam is not split into a sequence of pulses, but acts continually throughout the entire period of injection of the beam with chaotic modulation. The spectrum of emission created by such a beam at the input of the amplifier is rather ragged, as is clear from the diagram. From further discussion we shall see that the nature of amplification crucially depends on the method of primary modulation of the electron beam.

Figure 11 shows the spatial dynamics of the efficiency of modulation (7.12) and the absolute values of the amplitudes of the harmonics whose frequencies are closest to the wave – particle and wave – wave resonances (harmonics number 13 and number 18 for the parameters in question). Figure 11a corresponds to regular modulation of the beam, Fig. 11b to chaotic modulation. The results which follow from these diagrams are listed in Table 1.

Table 1. Characteristics of a Compton amplifier for different beam modulation modes.

Beam modulation	Saturation length, cm	Maximum efficiency, %; power, MW	Width of spectrum at half-height of the principal peak, 10^{10} rad s^{-1}
Regular	28	15; 160	8
Chaotic	16	23; 240	2.5

The last column in Table 1 contains data taken from Fig. 12, which shows the spectra and the phase planes at the amplification stage close to saturation for each of the modulation modes (regular in Fig. 12a and chaotic in Fig. 12b). Certain regularities catch the eye. The higher the

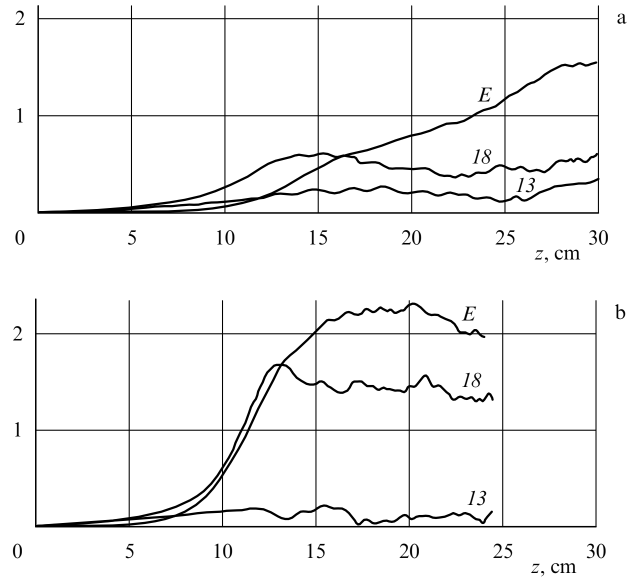

Figure 11. Spatial dynamics of the total efficiency of emission and the amplitudes of resonance harmonics for the Compton amplifier: (a) regular density modulation; (b) chaotic density modulation.

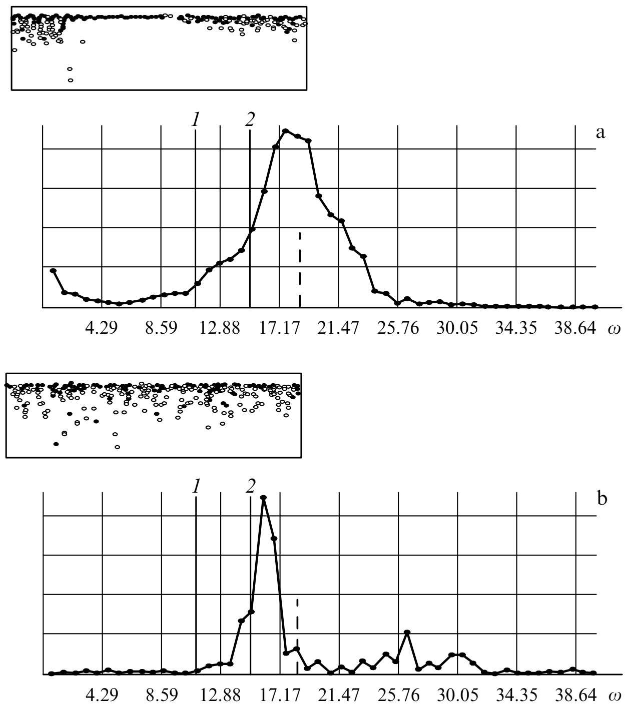

Figure 12. Spectral distributions at saturation stage for the Compton amplifier: (a) regular density modulation; (b) chaotic density modulation.

degree of chaotization of the input beam, the shorter the saturation length, the higher the maximum efficiency and power, the narrower the band of amplified frequencies. Obviously, the 'input beam' can be replaced by the more general term 'input signal'.

These regularities can be interpreted in the following manner. When the modulation of the beam is regular, then, as follows from Fig. 10a, a large number of modes, including those from the amplification range predicted by the linear theory (see curve b in Fig. 4), occur under approximately equal conditions. All these modes are amplified to form a relatively broad spectrum. Observe that the resulting spectrum presented in Fig. 12a contains components from regions not predicted by the linear theory: there are amplified modes from the high-frequency region, where the gain according to the linear theory is zero, and there are amplified modes at very low frequencies. This is probably the result of a nonlinear interaction between waves with close s numbers. Then, as follows from the phase diagram included in Fig. 10a, the field formed in the case of regular modulation of the beam is in the shape of localized packets which only act upon some of the beam electrons. Even at the resulting stage (see Fig. 12a) the beam exhibits weakly perturbed portions which are not affected by the still compact wave packets. Since not all electrons of the beam are involved in the interaction with the field, regular modulation corresponds to the greatest saturation length and the lowest efficiency of emission.

In the case of chaotic modulation the situation is different. The field is not split into a sequence of short pulses (see phase diagram in Fig. 10b), and so all the electrons of the beam take part in the interaction. As a consequence, the efficiency is higher, and the saturation length is shorter. The phase diagram in Fig. 12b shows that a large number of electrons are decelerated, which proves that most of the electrons of the beam interact with the plasma waves and give away part of their energy. Moreover, as follows from Fig. 10b the initial spectrum in case of chaotic modulation is ragged, and the amplification of waves starts in different conditions. The most efficiently amplified waves are those whose frequencies lie close to the maximum of the linear gain. This explains the narrow emission spectrum in the case of chaotic modulation.

Now let us consider the Raman amplifier based on the collective Cherenkov effect. The parameters remain the same, only the radius of plasma is increased to $r_{\mathrm{p}} = 1.1$ cm. The behavior of the gain for these parameters is shown in Fig. 5.

Figure 13 shows the space dependence of the efficiency of emission (7.12), and the absolute values of the amplitudes of the harmonics corresponding to the wave–wave (number *11*) and wave–particle (number *7*) resonances. The curves are plotted for the case of regular modulation. For other modulation modes the curves are similar. Actually, the mode of modulation of the beam is not important for the Raman amplifier, since in any case amplification occurs in a narrow band. In the case of regular modulation the local wave pulses smear out (that is, become monochromatized) in the initial stage. In the case of chaotic modulation regular (close to sinusoidal) structures are formed in the phase planes

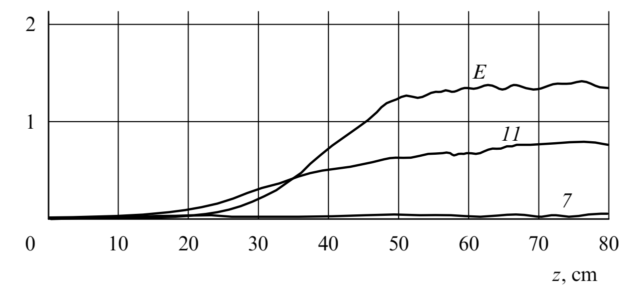

Figure 13. Spatial dynamics of the total efficiency of emission and the amplitudes of resonance harmonics for the Raman amplifier (regular density modulation).

corresponding to the interaction of the beam with a single mode. Thereafter the initial modulation ceases to be of any significance. Note the following:

— the maximum efficiency is about 14%;

— the maximum power is about 140 MW;

— the amplification saturation length is about 50 cm;

— the saturation results in a quasi-steady state, in which the highly thermalized beam (see below) and the amplified waves no longer interact on the average;

— the wave corresponding to the wave–particle resonance (harmonic number seven) is not amplified.

Figure 14 shows the spectra and the phase planes at the saturation stage in the Raman amplifier; Fig. 14a corresponds to regular modulation of the beam, and Fig. 14b to chaotic modulation. In the case of regular modulation the spectrum is not too narrow, but falls precisely into the range predicted by the linear theory (see Fig. 5). In the case of chaotic modulation the spectrum is extremely narrow: in fact, just one mode corresponding to the wave–wave resonance is amplified. In all cases the beam after saturation is highly chaotized (thermalized), as is clear from the phase diagrams in Fig. 14.

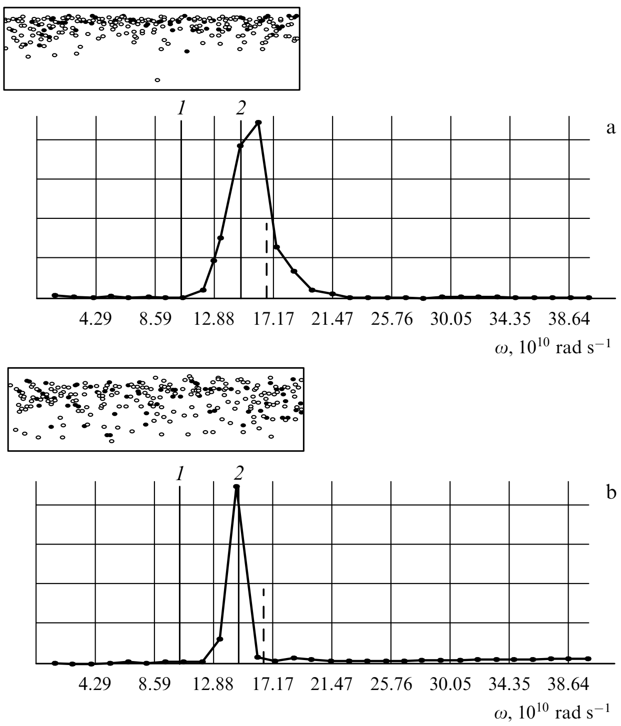

Figure 14. Spectral distributions at the saturation stage for the Raman amplifier: (a) regular density modulation; (b) chaotic density modulation.

Let us consider yet another amplification regime which occurs close to the plasma frequency limit. Inequality (4.15) is satisfied, but owing to the high current there is a narrow amplification band at very low frequencies. All parameters are the same as those of the Compton amplifier with $r_p = 0.8$ cm, but the plasma frequency is reduced to $\omega_p = 15 \times 10^{10}$ rad s^{-1}. The gain for these parameters is shown in Fig. 15. We see that the wave–particle resonance is not present, whereas the wave–wave resonance occurs at a very low frequency. As the plasma frequency is reduced further, the wave–wave resonance disappears, and soon the amplification disappears too.

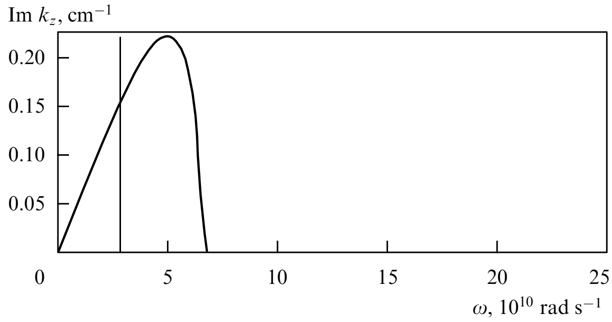

Figure 15. Gain factor for the Compton amplifier at low value of plasma frequency.

Figure 16 shows the spatial dynamics of the efficiency of amplification and the absolute values of the first and third harmonics. One may conclude that when the plasma frequency is close to the threshold, the efficiency of emission may be very high (up to 24%), and the output power may be as high as 250 MW. Figure 17 shows the emission spectrum. We see that the amplification is restricted to a very narrow waveband, corresponding to the maximum of the linear gain. In addition, there is a small peak in the spectrum of amplified waves at the doubled frequency, which may be attributed to the nonlinear generation of second harmonics of the beam charge density. The effect of amplification at the near-threshold plasma frequency may be useful for the construction of a low-frequency source of monochromatic radiation. The diagrams in Fig. 16 and 17 correspond to regular

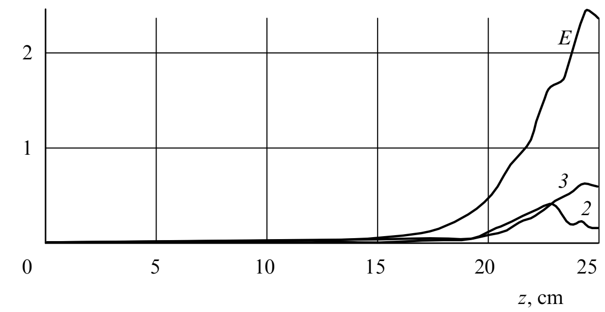

Figure 16. Spatial dynamics of the total efficiency of emission and the amplitudes of the second and third harmonics for the Compton amplifier at low values of plasma frequency and for regular density modulation of the beam.

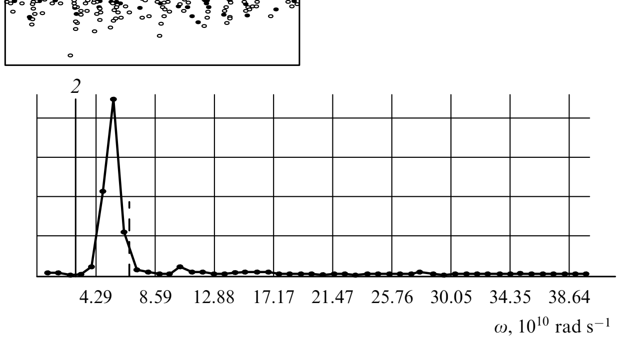

Figure 17. Spectral distributions at the saturation stage for the Compton amplifier at low values of plasma frequency and for regular density modulation of the beam.

modulation of the beam. Other modulation modes lead to similar results, but the above-noted effect remains: the more regular the modulation, the broader the spectrum and the lower the efficiency of emission.

9. Conclusion

Observe once again that all the particular results quoted in this review have been obtained for real objects of experimental study. The most important feature is that the theoretical predictions generally fit in well with the experimental results. This concerns such crucial characteristics as the threshold plasma frequency, the initial beam current, the emitted frequency range, the integral efficiency of emission, etc. There are certainly some difficulties associated mainly with the insufficiency of available experimental data on large-current relativistic plasma sources of microwave radiation. We hope that further experiments will provide a basis for a more comprehensive comparison, and we shall have the opportunity to discuss some problems which at present had to be left out of the discussion.

References

1. Bogdankevich L S, Rukhadze A A *Usp. Fiz. Nauk* **103** 609 (1971) [*Sov. Phys. Usp.* **14** 163 (1972)]
2. Bogdankevich L S, Kuzelev M V, Rukhadze A A *Usp. Fiz. Nauk* **133** 3 (1981) [*Sov. Phys. Usp.* **24** 1 (1981)]
3. Kuzelev M V et al. *Usp. Fiz. Nauk* **146** 709 (1985) [*Sov. Phys. Usp.* **28** 724 (1985)]
4. Kuzelev M V, Rukhadze A A *Usp. Fiz. Nauk* **152** 285 (1987) [*Sov. Phys. Usp.* **30** 507 (1987)]
5. Kuzelev M V, Rukhadze A A, Filippychev D S, in *Relyativistskaya Vysokochastotnaya Élektronika* (Relativistic High-Frequency Electronics) (Gorky: IPFAN SSSR, 1981) p. 170
6. Kuzelev M V et al., in *Relyativistskaya Vysokochastotnaya Élektronika* (Relativistic High-Frequency Electronics) (Gorky: IPFAN SSSR, 1983) p. 160
7. Kuzelev M V et al. *Fiz. Plazmy* **13** 1370 (1987) [*Sov. J. Plasma Phys.* **13** 793 (1987)]
8. Kuzelev M V, Rukhadze A A, in *Relyativistskaya Vysokochastotnaya Élektronika* (Relativistic High-Frequency Electronics) (Gorky: IPFAN SSSR, 1988) p. 7; in *Problemy Fiziki i Astrofiziki* (k 70-letiyu V L Ginzburga) [Problems of Physics and Astrophysics (70th anniversary of V L Ginzburg)] (Moscow: Nauka, 1989) p. 70
9. Rukhadze A A et al. *Fizika Sil'notochnykh Relyativistskikh Élektronnykh Puchkov* (Physics of Large-Current Relativistic Electron Beams) (Moscow: Atomizdat, 1980)
10. Kuzelev M V, Rukhadze A A *Élektrodinamika Plotnykh Élektronnykh Puchkov v Plazme* (Electrodynamics of Dense Electron Beams in Plasma) (Moscow: Nauka, 1990)
11. Akhiezer A I, Faĭnberg Ya B *Dokl. Akad. Nauk SSSR* **69** 555 (1949)
12. Bohm D, Gross E *Phys. Rev.* **75** 1851 (1949)
13. Faĭnberg Ya B *At. Energ.* **11** 313 (1961)
14. Faĭnberg Ya B *Usp. Fiz. Nauk* **93** 617 (1967) [*Sov. Fiz. Usp.* **10** 750 (1968)]
15. Bernashevskiĭ G A et al. *Plazmennye i Élektronnye Usiliteli i Generatory SVCh* (Plasma and Electron Microwave Amplifiers and Generators) (Moscow: Sovetskoe Radio, 1965)
16. Nezlin M V *Usp. Fiz. Nauk* **120** 481 (1976) [*Sov. Fiz. Usp.* **19** 946 (1976)]
17. Nezlin M V *Dinamika Puchkov v Plazme* (Dynamics of Beams in Plasma) (Moscow: Energoizdat, 1982) [*Physics of Intense Beams in Plasmas* (Bristol, Philadelphia: Inst. Physics Publ., 1993)]
18. Tajima T *Phys. Fluids* **22** 1157 (1979)
19. Aĭzatskiĭ N I *Fiz. Plazmy* **6** 597 (1980) [*Sov. J. Plasma Phys.* (1980)]
20. Kuzelev M V, Rukhadze A A *Pis'ma Zh. Tekh. Fiz.* **6** 1388 (1980) [*Sov. Tech. Phys. Lett.* **6** 597 (1980)]
21. Bogdanov V V, Kuzelev M V, Rukhadze A A *Fiz. Plazmy* **10** 548 (1984) [*Sov. J. Plasma Phys.* **10** 319 (1984)]
22. O'Neil T *Phys. Fluids* **8** 2255 (1965)
23. Onishchenko I N et al. *Pis'ma Zh. Eksp. Teor. Fiz.* **12** 407 (1970) [*JETP Lett.* **12** 281 (1970)]; *Plasma Phys.* **14** 591 (1972)
24. Kovtun R I, Rukhadze A A *Zh. Eksp. Teor. Fiz.* **58** 1709 (1970) [*Sov. Phys. JETP* **31** 915 (1970)]
25. Shapiro V D, in *Problemy Teorii Plazmy* (Problems of Plasma Theory) (Kiev: Naukova Dumka, 1972) p. 257
26. Trubetskov D I, Pishchik L A *Fiz. Plazmy* **15** 342 (1989) [*Sov. J. Plasma Phys.* **15** 200 (1989)]
27. Rukhadze A A *Vestn. Akad. Nauk SSSR* (1) 19 (1972)
28. Bogdankevich L S, Rukhadze A A, in *Problemy Teorii Plazmy* (Problems of Plasma Theory) (Kiev: Naukova Dumka, 1972) p. 210
29. Didenko A N, Grigor'ev V P, Usov Yu P *Moshchnye Élektronnye Puchki i Ikh Primenenie* (High-Power Electron Beams and Their Applications) (Moscow: Atomizdat, 1977)
30. Abramyan E A, Al'terkop B A, Kuleshov G D *Intensivnye Élektronnye Puchki* (Intensive Electron Beams) (Moscow: Energoizdat, 1984)
31. Kovalev N F et al. *Pis'ma Zh. Eksp. Teor. Fiz.* **18** 232 (1973) [*JETP Lett.* **18** 232 (1973)]; in *Relyativistskaya Vysokochastotnaya Élektronika* (Relativistic High-Frequency Electronics] (Gorky: IPFAN SSSR, 1979) p. 76
32. Carmal J, Friedman M, Raizer M *Phys. Rev. Lett.* **33** 1478 (1974)
33. Gaponov-Grekhov A V, Petelin M I *Vestn. Akad. Nauk SSSR* (4) 11 (1979)
34. Collected papers: *Relyativistskaya Vysokochastotnaya Élektronika* (Relativistic High-Frequency Electronics) Vyp. 1–6 (Gorky: IPFAN SSSR, 1979–1988); *Generatory Kogerentnogo Izlucheniya na Svobodnykh Élektronakh* (Generators of Coherent Radiation Based on Free Electrons) (Moscow: Mir, 1983)
35. Kuzelev M V et al. *Zh. Eksp. Teor. Fiz.* **83** 1358 (1982) [*Sov. Phys. JETP* **56** 780 (1982)]
36. Kuzelev M V et al. *Dokl. Akad. Nauk SSSR* **267** 829 (1982) [*Sov. Phys. Dokl.* **27** 1030 (1982)]
37. Selivanov I A et al. *Fiz. Plazmy* **15** 1283 (1989) [*Sov. J. Plasma Phys.* **15** 744 (1989)]
38. Rabinovich M S, Rukhadze A A *Fiz. Plazmy* **2** 715 (1976)
39. Bogdankevich L S, Rabinovich M S, Rukhadze A A *Izv. Vyssh. Uchebn. Zaved. Fiz.* **22** (10) 47 (1979) [*Sov. Phys. J.* **22** 1073 (1979)]
40. Bliokh Yu P et al. *Dokl. Akad. Nauk SSSR* **125** 56 (1982)
41. Shkvarunets A G, Rukhadze A A, Strelkov P S *Fiz. Plazmy* **20** 682 (1994)
42. Kuzelev M V et al. *Zh. Eksp. Teor. Fiz.* **109** 2048 (1996) [*JETP* **82** 1102 (1996)]
43. Kuzelev M V et al. *Zh. Eksp. Teor. Fiz.* **101** 460 (1992) [*Sov. Phys. JETP* **74** 242 (1992)]
44. Krasil'nikov M A, Kuzelev M V, Rukhadze A A *Zh. Eksp. Teor. Fiz.* **108** 521 (1995) [*JETP* **81** 280 (1995)]
45. Birau M et al. *Zh. Eksp. Teor. Fiz.* **111** 1258 (1997) [*JETP* **84** 694 (1997)]
46. Kuzelev M V, Rukhadze A A *Fiz. Plazmy* **23** (10) (1997) (in press)
47. Aleksandrov A F et al. *Zh. Tekh. Fiz.* **50** 2381 (1980) [*Sov. Phys. Tech. Phys.* (1980)]
48. Abubakirov É B et al. *Pis'ma Zh. Tekh. Fiz.* **9** (9) 533 (1983) [*Sov. Tech. Phys. Lett.* **6** 400 (1983)]
49. Bondar' Yu F et al. *Fiz. Plazmy* **9** 383 (1983) [*Sov. J. Plasma Phys.* (1983)]
50. Voronkov S N, Loza O T, Strelkov P S *Fiz. Plazmy* **17** 751 (1991); **19** 601 (1993)
51. Kuzelev M V, Panin V A *Fiz. Plazmy* **19** 732 (1993) [*Plasma Phys. Rep.* **19** 376 (1993)]
52. Kuzelev M V, Panin V A, Plotnikov A P *Fiz. Plazmy* **17** 1459 (1991) [*Sov. J. Plasma Phys.* (1991)]
53. Kuzelev M V et al. *Dokl. Akad. Nauk SSSR* **300** (5) 1112 (1988) [*Sov. Phys. Dokl.* **33** 444 (1988)]
54. Dorofeenko V G, Krasovitskiĭ V B, Fomin G V *Zh. Eksp. Teor. Fiz.* **98** 419 (1990) [*Sov. Phys. JETP* **71** 234 (1990)]
55. Kuzelev M V et al., in *Trudy IOFAN* (IOFAN Proceedings) Vol. 45 (Moscow: Nauka, 1994) p. 17
56. Katsenelenbaum B Z *Vysokochastotnaya Élektrodinamika* (High-Frequency Electrodynamics) (Moscow: Nauka, 1966)
57. Born M, Wolf E *Principles of Optics* (Oxford, New York: Pergamon Press, 1965) [Translated into Russian (Moscow: Nauka, 1970)]

58. Akhiezer A I (Ed.) *Élektrodinamika Plazmy* (Electrodynamics of Plasma) (Moscow: Nauka, 1974)
59. Libov R *Vvedenie v Teoriyu Kineticheskikh Uravneniĭ* (Introduced to Kinetic Equalization Theory) (Moscow: Mir, 1974)
60. Kuzelev M V, Rukhadze A A *Izv. Vyssh. Uchebn. Zaved. Radiofiz.* **36** (10) 867 (1993) [*Radiophys. Quantum Electron.* **36** 661 (1993)]
61. Kuzelev M V, Mukhametzyanov F Kh, Shkvarunets A G *Fiz. Plazmy* **9** 1137 (1983) [*Sov. J. Plasma Phys.* **9** 655 (1983)]
62. Aleksandrov A F, Kuzelev M V, Khalilov A N *Zh. Eksp. Teor. Fiz.* **93** (5/11) 1714 (1987) [*Sov. Phys. JETP* **66** 978 (1987)]
63. Kadomtsev B B, Mikhaĭlovskiĭ A B, Timofeev A V *Zh. Eksp. Teor. Fiz.* **47** 2266 (1964) [*Sov. Phys. JETP* **20** 1517 (1965)]
64. Fedosov A I et al. *Izv. Vyssh. Uchebn. Zaved. Fiz.* (10) 134 (1977)
65. Belomytsev S Ya et al. *Fiz. Plazmy* **7** 86 (1981) [*Sov. J. Plasma Phys.* (1981)]
66. Birau M *Phys. Rev. E* **54** (5) 5599 (1996)
67. Birau M et al. *ICPIG, 1997* (Touluza, 1997) (in press)